RRFM IGORR 2007

LYON, France 11.3. - 15.3. 2007

Transactions

11th International Topical Meeting

Research Reactor Fuel Management (RRFM)
and
Meeting of the International Group on Reactor Research (IGORR)

Centre de Congrès, Lyon, France
11– 15 March 2007

Organised by the
European Nuclear Society (ENS)

and

IGORR: International Group on Research Reactors

in co-operation with the
International Atomic Energy Agency (IAEA)

© 2007
European Nuclear Society
Rue de la Loi 57
1040 Brussels, Belgium
Phone + 32 2 505 30 54
Fax +32 2 502 39 02
E-mail ens@euronuclear.org
Internet www.euronuclear.org

These transactions contain all contributions submitted by 9 March 2007.

The content of contributions published in this book reflects solely the opinions of the authors concerned. The European Nuclear Society is not responsible for details published and the accuracy of data presented.

Session V

Innovative Methods in Research Reactor Physics

SESSION V - INNOVATIVE METHODS IN RESEARCH REACTORS PHYSICS

MCNPX 2.6.C VS. MCNPX & ORIGEN-S: STATE OF THE ART FOR REACTOR CORE MANAGEMENT	**5**
SIMULATION OF IRRADIATION OF A BUNDLE OF MOX FUEL RODS IN THE OMICO EXPERIMENT IN BR2	**10**
DETERMINING MTR RIA LIMITS USING EXPERIMENTAL DATA	**15**
SAFETY ANALYSIS OF RESEARCH REACTORS WITH BEST ESTIMATE COMPUTATIONAL TOOLS	**22**
KINETIC PARAMETERS CALCULATION AND MEASUREMENTS DURING THE OPAL COMMISSIONING	**27**
DETERMINATION OF SAFARI-1 NEUTRON FLUXES BY MCNPX MODELLING OF FOIL EXPERIMENTS	**32**
SOPHISTICATED MCNP CALCULATION OF THE FLUX MAP OF FRJ-2 USING A FULLY NODALIZED MODEL	**36**

MCNPX 2.6.C vs. MCNPX & ORIGEN-S: State of the Art for Reactor Core Management

S.KALCHEVA and E.KOONEN

SCK•CEN, Belgium Nuclear Research Centre
Boeretang 200, B-2400 MOL-Belgium

ABSTRACT

This paper discusses the application of the Monte Carlo burnup code MCNPX 2.6.C for the criticality and depletion reactor core analysis of the Material Testing Research Reactor BR2 in Mol, Belgium. A comparison with the developed at the BR2 reactor department combined MCNP&ORIGEN-S fuel depletion method is presented. The accuracy of the both methods, the consumption of the calculation time, the depletion capabilities, the advantages and disadvantages of use of the both methods are discussed. Validation of MCNPX 2.6.C is performed on the reactivity measurements at the Reactor BR2.

.

1. Introduction

In this paper we discuss the application of the Monte Carlo burnup code MCNPX 2.6.C [1] for the reactor core management of major reactor systems. The code MCNPX 2.6 is an extended version of the code MCNPX 2.5.0 and includes new depletion/burnup capabilities. At the present time MCNPX 2.6 is under active development and the latest versions of the code (A,B,C,….) are available to beta testers under a Beta Test Agreement. The code is tested mostly on simple reactor core models, represented by a single or few fuel assemblies. In this paper we present results of testing of the code on the whole core of complex heterogeneous system – such as the core of the Material Testing Reactor BR2 in SCK•CEN, in Mol, Belgium. A comparison with the combined MCNP&ORIGEN-S method [2] for reactor core physics analysis is presented. Validation of the code MCNPX 2.6.C is performed on the reactivity measurements at Reactor BR2. The detailed full scale 3-D heterogeneous geometry model of the reactor BR2 is used in the calculations.

2. MCNP&ORIGEN-S depletion methodology

The depletion calculations are performed using the burn up code ORIGEN-S [3]. It is a module of the SCALE system, which can be used in combination with other modules of the SCALE or it can be used as a stand-alone module as it is in the presented here calculations. The ORIGEN-S nuclear data libraries contain cross sections and fission yields for LWR. MCNPX is used for calculations of the continuous energy reaction rates and fluxes, which are converted into one – group constants. The MCNP calculated effective microscopic cross sections $<\sigma>_{eff}$ for the main actinides, dominant and some non dominant fission products of the HEU fuel, weighted in the spectrum of the needed fuel region j, are used to update the existing cross sections for the LWR reactor in the ORIGEN-S libraries (see Table I). The input for ORIGEN-S can be the fission power or the neutron flux, calculated by MCNP in the spatial cells where the burnup calculations are needed. ORIGEN-S evaluates the evolution of the isotopic fuel densities for the desired number depletion time steps. The isotopic fuel composition for a given time step is introduced back into the MCNP model and distributed in the core using the detailed 3–D power peaking factors, which are earlier evaluated with MCNP [2]. The comparison of the depletion methodologies by MCNPX 2.6.C and MCNPX&ORIGEN-S method is schematically presented at Fig. 1.

Table I. MCNPX calculation of effective thermal microscopic cross sections in typical fuel channel of the reactor BR2, which are used to update the existing cross sections in the ORIGEN-S libraries for

LWR. The cross sections data from the files ENDF/B-V,VI are used in the calculations of $<\sigma>_{eff}$ [barn] by MCNPX.

Nuclide	$<\sigma>_{therm}^{ORIGEN-S}$	$<\sigma>_{therm}^{MCNPX}$	Nuclide	$<\sigma>_{therm}^{ORIGEN-S}$	$<\sigma>_{therm}^{MCNPX}$
^{235}U (n,γ)	98	68	^{103}Rh (n,γ)	150	113
^{235}U (n,f)	520	400	^{105}Rh (n,γ)	1.8E+04	1.2E+04
^{238}U (n,γ)	2.73	2	^{135}Xe (n,γ)	3.6E+06	2.2E+06
^{238}U (n,f)	0	8E–06	^{147}Pm (n,γ)	235	127
^{237}Np (n,γ)	170	153	^{149}Sm (n,γ)	4.15E+04	5.5E+04
^{237}Np (n,f)	0.019	0.013	^{150}Sm (n,γ)	102	72
^{239}Pu (n,γ)	632	360	^{151}Sm (n,γ)	1.5E+03	8.3E+03
^{239}Pu (n,f)	1520	750	^{152}Sm (n,γ)	210	150

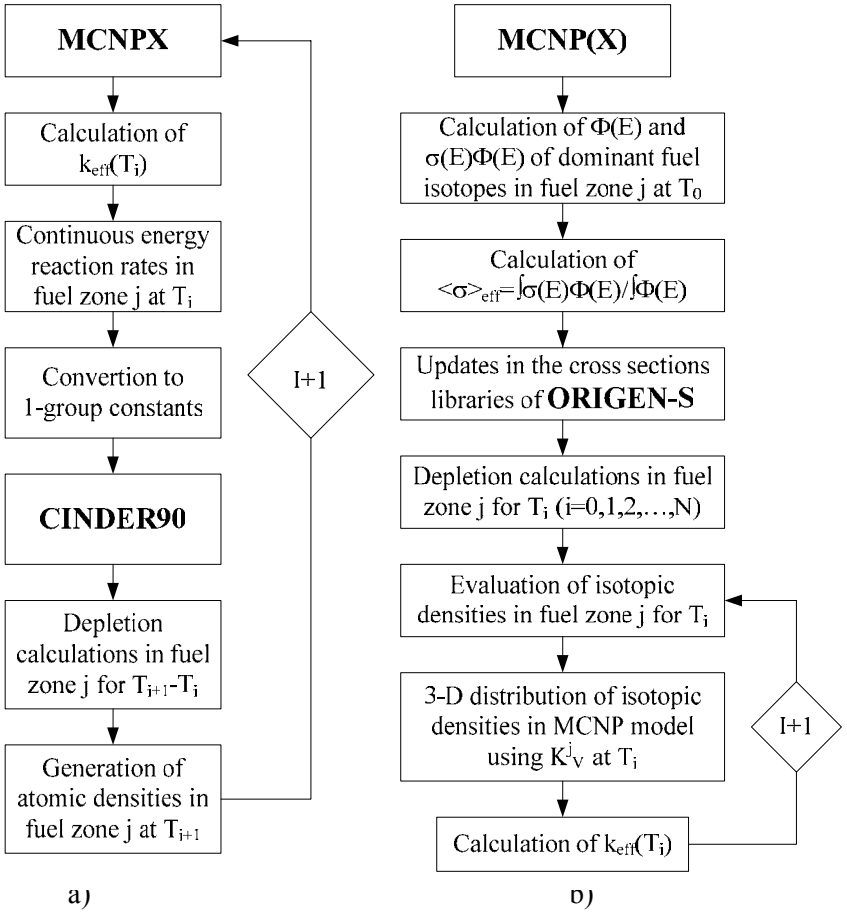

Figure 1. Comparison of depletion methodologies by: a) MCNPX 2.6 and b) MCNP&ORIGEN-S.

3. MCNX 2.6 depletion methodology

The depletion/burnup capability in MCNPX is based on the 1 – D burnup code CINDER90 [1] and Monte Burns [1]. The MCNPX depletion process internally links the steady – state flux calculations in MCNPX with the isotopic depletion calculations in CINDER90. MCNPX runs a steady – state calculation to determine the effective multiplication factor k_{eff}, 63 – group fluxes and continuous energy reaction rates for (n,gamma), (n,f), (n,2n), (n,3n), (n,alpha) and (n,p), which are converted into one – group constants and used by CINDER90 to carry out the depletion calculations and to generate new number densities for the next time step. MCNPX takes those new number densities for the corresponding fuel cells and generates another set of fluxes, reaction rates. The process is automatic and repeats itself for each time step until the requested final time step. The calculated MCNPX 63 – energy group fluxes in combination with the inherent 63 – group cross sections of CINDER90 are used to determine the rest of the interaction rates, which are not calculated by MCNPX.

4. Testing of MCNPX 2.6.C on the Research Reactor BR2

The burnup code MCNPX 2.6.C is tested on the Reactor BR2. Depletion and eigenvalue calculations are performed for the full scale 3-D heterogeneous geometry model of the reactor, which describes the real reactor core of BR2 in a form of a twisted hyperboloidal bundle [2]. The evolutions of the macroscopic, effective microscopic cross sections and atomic densities are evaluated using CINDER90 and compared with ORIGEN-S.

4.1. Evolution of macroscopic cross sections by MCNPX 2.6

The evolutions of the macroscopic cross sections of the main actinides, burnable absorbers, and fission products were performed for the fresh fuel elements, which have been irradiated during 5 operating cycles with shutdowns ~ 20 days and without core reloading (see Fig. 2). It was obtained that the major contributions into the negative reactivity of the core give the burnable absorbers ^{10}B and ^{149}Sm in the fresh fuel. For the burnt fuel the main contributors into the negative reactivity are ^{149}Sm and ^{10}B at BOC and ^{135}Xe during the cycle and at EOC, which is in accordance with the results in Table II [2]. Among the non dominant F.P. the most contributions come from ^{103}Rh, ^{147}Pm, ^{151}Sm, ^{152}Sm. All other non dominant isotopes have been evaluated, but their Σ are less than 0.0005 cm^{-1}.

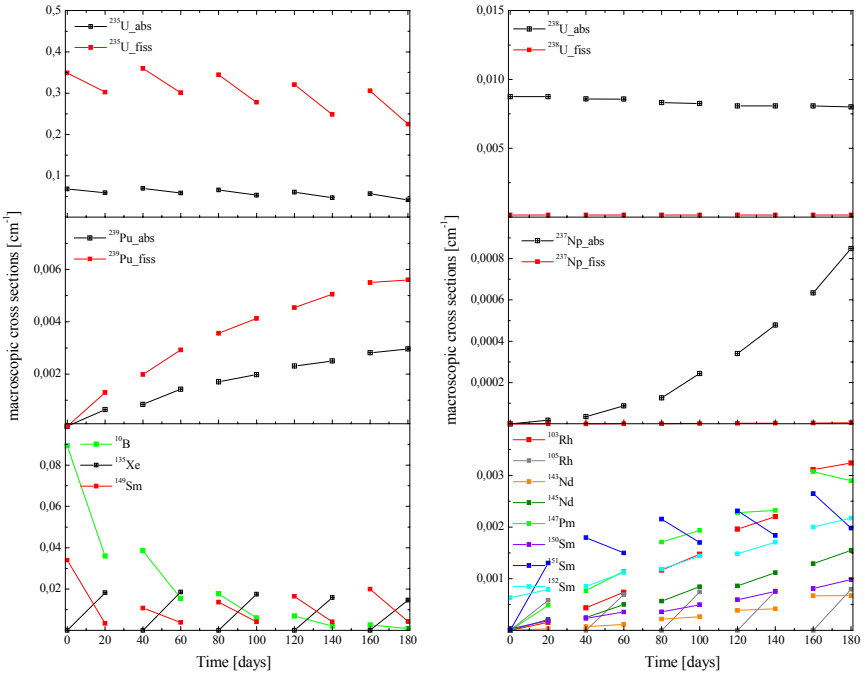

Figure 2. Evolution by MCNPX 2.6.C (CINDER90) of the macroscopic cross sections of the main actinides, burnable absorbers and dominant F.P. during 5 operating cycles (shown are data only for BOC and EOC).

4.2. Comparison of the atomic densities by CINDER90 and ORIGEN-S

The final goal of this study was to compare the depletion and criticality capabilities of the new burn up Monte Carlo code MCNPX 2.6.C with those of the combined MCNP&ORIGEN-S method. The evolutions of the isotopic fuel densities of the HEU fuel are evaluated by CINDER90 and by ORIGEN-S and compared at Fig. 3. As can be seen and as it was expected the evolutions of the masses of major fissile actinides and dominant F.P. are similar, because the both methods use the calculated reaction rates by the same Monte Carlo method, i.e. MCNP, which are further introduced into the one – group depletion equation.

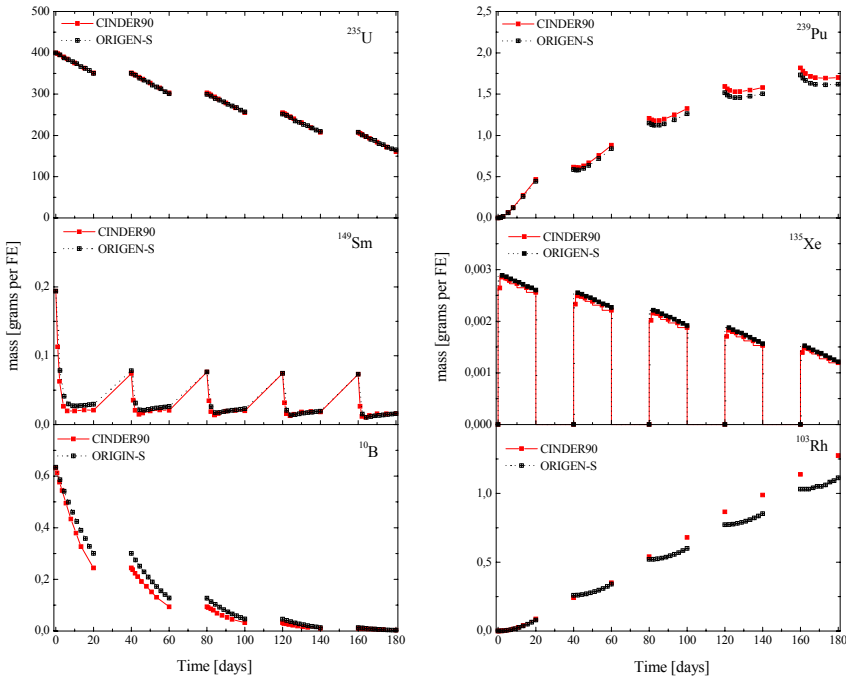

Figure 3. Time evolution of fissile isotopes and dominant F.P. in HEU (90% ^{235}U) fuel

4.3. Criticality calculations by MCNPX 2.6 and MCNP&ORIGEN-S

Finally, k_{eff} and the reactivity evolutions during an operation cycle have been evaluated by the both methods and validated on the reactivity measurements of the reactor BR2. The calculation procedure by MCNPX 2.6.C includes automatic calculation of k_{eff} and nuclide inventory by CINDER90 at each depletion time step. The reactivity calculations by the combined MCNP&ORIGEN-S method are performed in the following manner: the effective microscopic cross sections for major fissile actinides, dominant and some of the non dominant F.P. are evaluated with MCNP at BOC and used by ORIGEN-S to evaluate the isotopic fuel densities for all needed depletion time steps. After that the isotopic fuel composition for a given depletion step is introduced back into the MCNP model and distributed in the core using the preliminary calculated with MCNP 3 – D power peaking factors [2]. The k_{eff} is calculated for the relevant time step (see Fig. 4a). The calculations by both methods can be performed at the same critical position of CR bank at BOC. After that the reactivity value for each time step (Fig. 4b) together with the calculated earlier differential CR worth (Fig. 4c) are used to evaluate the positions Sh of the CR bank during the operating cycle (Fig. 4d). The comparison of the reactivity evolutions and CR motion during the cycle determined by the both methods has shown an acceptable agreement with the experimental values (see Fig. 4b, 4d).

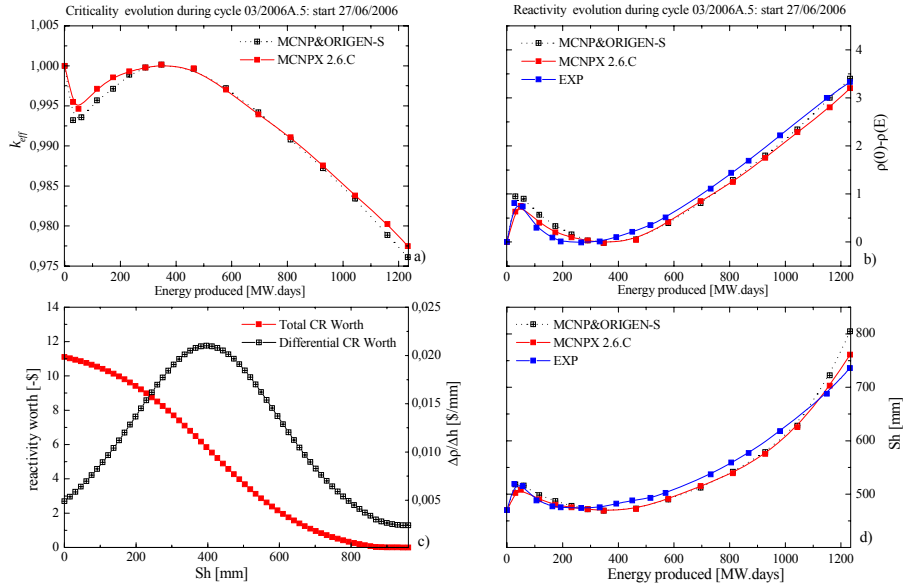

Figure 4. a) Evolution of k_{eff} ; b) Reactivity evolution; c) Total and Differential CR Worth; d) Motion of the Control Rods bank during cycle 03/2006A.5 of BR2.

5. Conclusions

The capabilities for depletion and criticality reactor core analysis of the new burnup Monte Carlo code MCNPX 2.6.C are compared with those of the combined MCNPX&ORIGEN-S method for the reactor BR2. The both methods use the same Monte Carlo code, which is linked with a 1 – D depletion code: CINDER90 in MCNPX 2.6 and ORIGEN-S in the MCNP(X)&ORIGEN-S method. In the both methods the reaction rates are calculated by MCNP(X) and the one – group constants are introduced into the depletion equation. The difference is that in MCNPX 2.6.C the whole process is automatic and the steady – state flux calculations by MCNPX in the requested fuel region are internally linked with the depletion calculations by CINDER90. Therefore the reaction rates are updated for each time step in the requested fuel region during the irradiation period. In the MCNP&ORIGEN-S method the reaction rates are calculated by MCNP once – at BOC and introduced into ORIGEN-S, which performs the depletion calculations for all desired time steps. Then the isotopic fuel composition for a given time step is introduced back into the MCNP geometry model and distributed in the core using the calculated earlier 3 – D power peaking factors, and the k_{eff} is evaluated. The same procedure is repeated for each time step, so that the different depletion steps can be calculated independently and simultaneously, which saves a lot of computational time. The number of the fuel depletion zones used in the MCNP&ORIGEN-S method is about 4000. Although the number of the fuel cells, in which the material can be burnt is unlimited in the latest version MCNPX 2.6.C, in practice, for a complex heterogeneous system, the number of the spatial fuel zones, which can be depleted is still limited by the allowed computer memory. The accuracy of the criticality calculations by MCNPX 2.6.C is still lower in comparison with the validated on many experimental results MCNP&ORIGEN-S method. However, the development of the code MCNPX 2.6 is a dynamic process, and each higher version of the code is an improved variant of the previous one….

6. References

[1] MCNPX, Version 26C, John S. Hendricks et al., LANL, LA-UR-06-7991. December 7, 2006.

[2] S.Kalcheva, E.Koonen and B.Ponsard, "Accuracy of Monte Carlo Criticality Calculations During BR2 Operation," *Nucl. Technol.*, **151**, 201 (2005).

[3] ORIGEN-S: SCALE System Module to Calculate Fuel Depletion, Actinide Transmutation,Fission Product Buildup and Decay, and Associated Radiation Terms, Oak Ridge National Laboratory, NUREG/CR-0200, Revision 5. ORNL/NUREG/CSD-2/V2/R5, March 1997.

SIMULATION OF IRRADIATION OF A BUNDLE OF MOX FUEL RODS IN THE OMICO EXPERIMENT IN BR2

V.KUZMINOV

SCK•CEN, Boeretang 200, B-2400 – Belgium

ABSTRACT

A description of the calculation method which was applied for the simulation of the irradiation history of an assembly of different MOX fuel rods in the BR2 is given in the paper. The Monte Carlo simulation of irradiation experiment (OMICO) consisting of 16 MOX rods of different fuel compositions and assembled into two separated bundles one over other and loaded into one of the in-pile sections of the PWR simulation loop in BR2 was performed using the BR2 model with an interface module linking the input data for the MCNP and SCALE codes. The results of a direct Monte Carlo simulation are compared with the results of online thermal balance measurements of the power distribution in the IPS1 in-pile section comprising the OMICO bundles. In most cases the difference between the experimental and calculated values is less than 7-10%.

1. Introduction

The experimental program in the Belgian High Flux Materials Testing Reactor BR2 includes irradiation of different materials and of new types of nuclear fuel, radio-isotopes production, neutron transmutation doping of Si, et. al. The monitoring of irradiation conditions in IPS channels of BR2 includes on-line measurement of the thermal power using the thermal balance method implemented in the data acquisition system BIDASSE. This method permits to perform on-line measurement of absolute values of the deposited heating energy in the IPS channels. However, the detailed distribution of the power density inside the channel can be obtained using only the preliminary calculated relative distributions of power in all structural elements in the channel. Supplementary control of neutron fluxes inside the channel using self-powered neutron detectors was developed by L.Vermeeren and incorporated into BIDASSE system. The absolute values of the calculated power and temperature distributions in the IPS channels strongly depend on the reactor core load and on the reactor power history during the operation cycle. The maximum allowed deviation from the requested power density in the irradiated fuel rods is 10%, our goal is to limit this deviation to less than 5%. A post irradiation examination of the fission products distribution in the rods is used to reconstruct 'a posterior' the distribution of fission events density in the fuel rods and consequently of the energy deposition.

In the present paper we focus on the approach used to simulate and predict power and burn-up distributions in different complex fuel assemblies. In particular, we consider a bundle of different MOX fuel rods grouped into 2 segments one over other and containing 16 fuel rods of different fuel compositions in the OMICO experiment. One group of the fuel rods was equipped with detectors placed inside fuel rods to allow online measurements of temperature and pressure.

The general view on the 3-D MCNP model used in the calculations is shown in Fig.1. Orientation of the fuel rods OMICO in the channel IPS1 is shown in left Fig.1. In the right Fig.1 the position of the IPS1 channel is marked by red-blue colours in the reactor core cut.

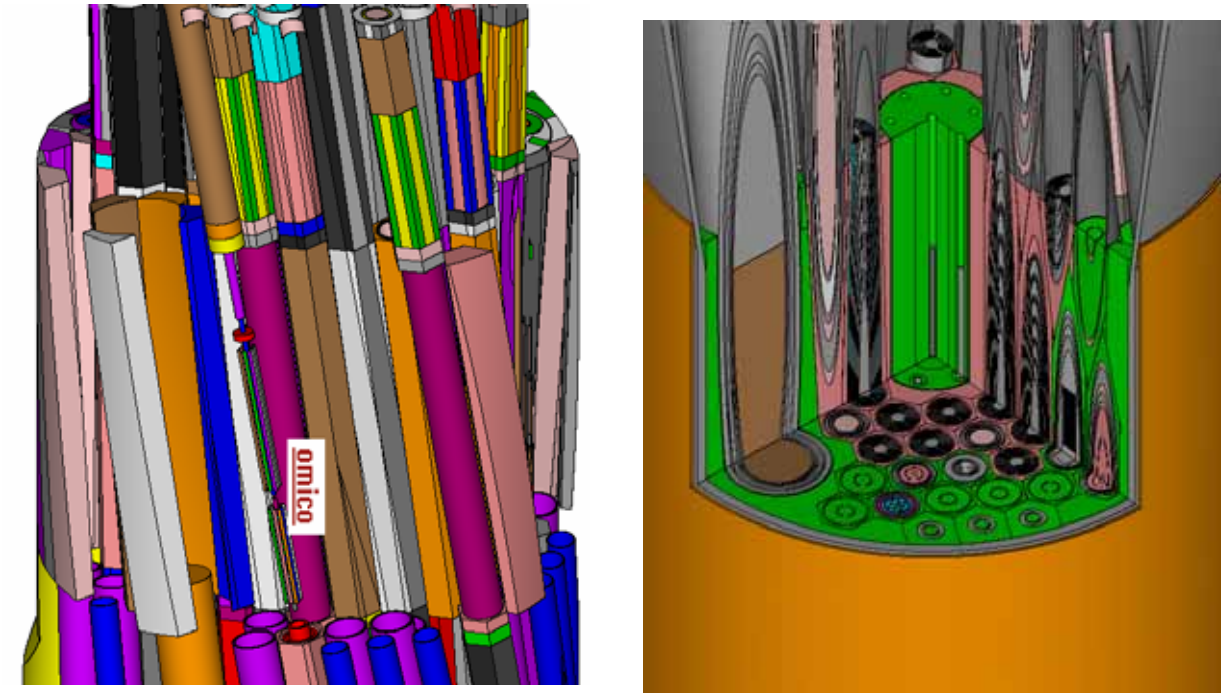

Fig 1. General view of inclined channels and a reactor core cut in MCNP 3-D model of the BR2. Two fuel bundles grouping of 8 MOX fuel rods each are shown in the left figure, while IPS1 channel (marked by red-blue colours) can be seen in the right figure of the BR2 core.

Each bundle includes of experimental fuel rods of different type, different initial enrichment and different fuel composition. Moreover, each bundle contains fuel pellets of different geometrical form: annular or solid fuel pellets. During the 7 irradiation cycles the environment near the position of the experiment was changed several times to satisfy all requested irradiation conditions in BR2. Examples of channels arrangement in different irradiation cycles near the position of the IPS1 channel are shown in Fig.2. In the last two cycles one bundle of MOX rods in IPS1 was replaced by dummy steel rods, while the irradiation of second bundle continued.

2. Calculation of fuel burn-up distribution in fuel rods

Accurate prediction of the fuel burn-up distribution and of the change of fissile nuclides concentration in the fuel element is important for maintaining the requested power and irradiation conditions in the tested fuel elements. However, it is difficult to perform a direct calculation of the detailed fuel burn-up distributions using the Monte Carlo codes in small parts of the fuel element irradiated in different positions in the reactor core. In practice the mean fuel burn-up in the fuel elements is calculated using average neutron fluxes inside fuel elements (sometimes in small numbers of fuel zones). This simplified approach permits to predict accurately an irradiation history of the fuel elements in the reactor core. However, detailed information about the spatial distribution of the fuel burn-up in the fuel elements cannot be obtained in this way.

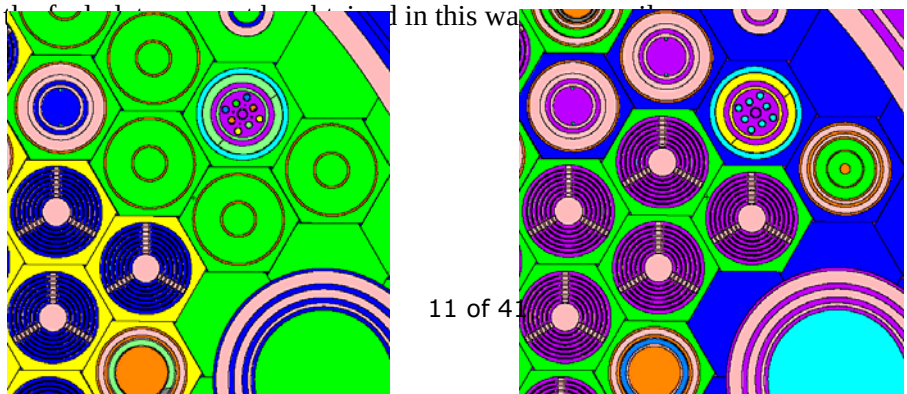

Fig.2 Examples of channels arrangement in different irradiation cycles near the IPS1 channel containing OMICO rods.

The fuel burn-up history and the change of fuel composition in the local fuel zone can be calculated using the mean values of the burn-up in the fuel element (rod, plate) and using the distributions of power peaking factor. The regular meshes of registration cells, $\{v\}_n$ {n=1,N}, are created in fuel elements for this purpose.

The dependence of the fuel burn-up, $\beta(v,T)$ expressed as the ratio of burned fissile atoms in the registration cell $\{v\}_n$ to their initial concentration, versus the energy released in fuel zone at the end of fuel cycle T is determined as

$$\beta(v,T) = C_v \frac{\int_0^T P(v,t)\,dt}{M(v)} 100\%, \qquad C_v = \frac{A_U}{N_A E_{eff}} \alpha_v, \qquad \alpha_v = \frac{\langle \sigma_f + \sigma_c \rangle_v}{\langle \sigma_f \rangle_v}$$

where A_U is the atomic mass number of the fissile element, N_A is the Avogadro constant, E_{eff} is the effective fission energy, $M(v)$ is the weight of the fuel in the cell $\{v\}$ in the beginning of the irradiation period and $P(v,t)$ is the power at the time t. Writing similar expression for the mean burn-up in the whole fuel element , we can find the dependence of the local burn-up $\beta_v(T_N)$ versus the mean burn-up, $\bar{\beta}(T_N)$, in the fuel rod after the N^{th} irradiation cycle, and versus the change of the specific power peaking factors $k_v(T_i)$ during the irradiation.

After N irradiation cycles (duration of N cycles is T_N) the local fuel burn-up, $\beta_v(T_N)$, after T_N irradiation time in each fuel zone $\{v\}$ can be calculated

$$\beta_v(T_N) = \beta_v(T_1) + \sum_{i=2}^{N} \left(\bar{\beta}(T_i) - \bar{\beta}(T_{i-1})\right) \times k_v(T_i) =$$

$$\sum_{i=1}^{N-1} \bar{\beta}(T_i)\left[k_v(T_i) - k_v(T_{i+1})\right] + \bar{\beta}(T_N) k_v(T_N),$$

The mean fuel burn-up in the whole fuel rod (element) can be calculated for the mean operation power using the SCALE or ORIGEN codes. The dependence of the nuclide composition versus the energy deposition (or equivalently on the fuel burn-up) in the fuel rod (element) can be calculated only once and be kept in the form of a burn-up data bank. These data are used each time when it is necessary to obtain the fuel composition for the local burn-up in the registration mesh.

In the approach presented here it is not necessary to solve the burn-up equation in each registration zone. The only what is necessary is to calculate the detailed distribution of the power peaking factors on the registration mesh. After that the distributions of the power peaking factors, k_v, are used to obtain the distributions of the fuel burn-up in registration cells. The nuclide composition in the registration cell for the obtained fuel burn-up can be taken from the burn-up data bank containing the dependence of the fuel composition on the fuel burn-up.

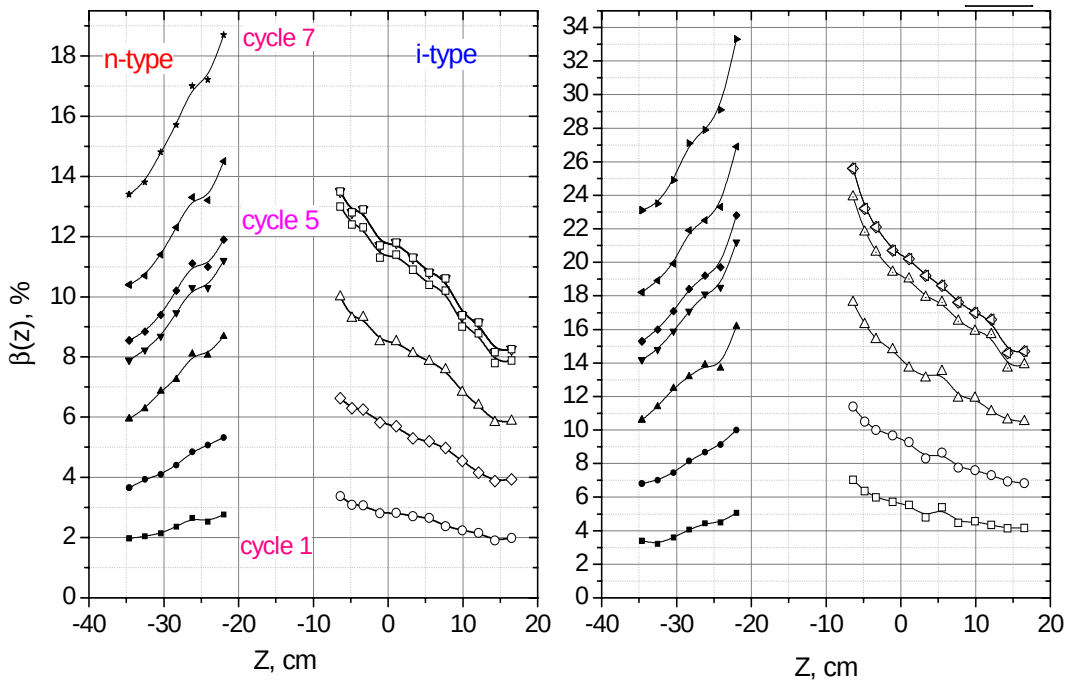

Fig.3 Example of spatial distributions of fuel burn-up in different fuel rods obtained for the scenario of several irradiation cycles.

The distributions of fuel burn-up in all 16 OMICO rods in 7 irradiation cycles was calculated using the described approach in automatic interface module linking input data for MCNP and SCALE codes. Because of a strong axial non-uniformity of neutron fluxes in the BR2 core and due to segmentation of rods, the distributions of the fuel burn-up are very non-uniform, see example in Fig.3. In the 'i'- type of fuel rods the local burn-up can vary from 13% to 34%, and in the 'n'-type can vary in the range of 8% - 26% (relative the initial concentration of fissile nuclide).

3 Comparison of calculated power history in the IPS1

Nuclear heating induced by prompt and delayed photons in structural materials of IPS1 channel amounts in average to about 20% of the total heating power in the channel comprising MOX fuel rods. The energy deposition from prompt photons produced in fission and neutron capture reactions in the reactor core was calculated using the MCNP model of BR2. The fraction of an energy deposited by delayed photons was estimated in a separate step. The spectrum and the intensity of the delayed photons from fission products were calculated using the SCALE-4.4a code, for example, in SAS2H (depletion analysis) module. The obtained spectrum of delayed photons was used as an external source of photons distributed in fuel elements in the BR2 core. Additional MCNP calculation of photon transport was performed with a new external source of delayed photons. The deposited heating energy E_γ^{SCALE} induced by the delayed photons was normalised per total intensity $\mathbf{I_\gamma}$ of delayed photons produced in BR2 fuel elements

$$E_\gamma^{SCALE} = n_\gamma \bar{E}_\gamma = \frac{I_\gamma \bar{E}_\gamma E_{fiss} 1.6\times10^{-19}}{P_{FE}} MeV\ /\ fiss$$

where the effective fission energy is equal to E_{fiss}=200 MeV/fission, n_γ is the number of delayed photons, and $\bar{E}_\gamma$ is the mean energy of photons. Normalizing the energy released with delayed photons in ^{235}U to E_γ= 7.2±1.1 MeV/fiss [1] we can obtain the intensity of delayed photons I_γ or the mean energy $\bar{E}_\gamma$ of delayed photons. These values were used to normalize the calculated heating energy in

IPS1 for the case with the external source of 'delayed photons' in MCNP code. The calculated heating energy in the IPS1 as was estimated is equal to 20.4-22.1 kW at the nominal power of BR2 reactor.
The comparison of the calculated power with the direct measurements became possible when measurements of the total energy induced by gammas in the IPS1 channel were performed by the thermal balance method. The measured energy was determined from several sets of measurements and equal to 20.7-21.2 kW. The difference between the calculated and measured gamma deposition power in the channel is less than 6%.
The total heating energy in the IPS1 with OMICO MOX rods in 7 irradiation cycles was calculated taking into account the axial profile of the fuel burn-up in all 16 rods. Comparison of power calculations with the on-line measured power in the IPS1 in each cycle was possible due to BIDASS system in BR2. The comparison of calculated and measured total power is included in Table 1. The difference in average is less than -5%, while for the first cycle is about 12%.

Table 1. Comparison of the calculated and measured thermal power in the IPS1 channel containing 16 MOX rods.

cycle	Time	BR2 reactor	IPS1 channel		
		Power, MW	Calculated power (C), kW	Measured power (M), thermal balance, kW	Difference (1-C/M), %
1	BOC	46	80	91	-12
	EOC	52	90	103	-13
2	BOC	61	80	86	-7
	EOC	60	89	89	+0
3	BOC	56	73	77	-5
	EOC	56	82	81	+2
4	BOC	57	72	74	-3
	EOC	57	77	82	-6
5	BOC	60	71	70	+2
	EOC	60	76	73	+4
6	BOC	58	36	38	-4
	EOC	58	37	35	+6
7	BOC	58	50	52	-4
	EOC	58	47	53	-11
mean					-4

4. Conclusion

In the present paper a simple approach for the calculation of detailed distribution of fuel burn-up was applied to bundles of different MOX fuel rods. The calculated power in the irradiation channel containing MOX rods was compared with the results of on-line measurements of the total power. The accuracy of calculations for most irradiation cycles is less than -10% and in average is about -4%. Preliminary comparison of the calculated number of fission reactions in the rods after the 1st irradiation cycle has revealed a small systematic deviation from the measured values.

5. References

[1] J.F.Breismeister ,"MCNP™ – A General Monte Carlo N-Particle Transport Code.Version 4c", LA-13709-M (2000).
[2] SCALE 4.4a, NUREG/CR-0200, Revision 6, ORNL/NUREG/CSD-2/V2/R.
[3] M.F.James, Energy Released in Fission, J.of Nucl.Energy, v.23,p517, 1969.

DETERMINING MTR RIA LIMITS USING EXPERIMENTAL DATA

S.E. DAY
McMaster Nuclear Reactor, McMaster University
1280 Main Street West, L8S 4K1 Hamilton, Ontario – Canada
dayse@mcmaster.ca

ABSTRACT

Reactivity initiated accidents (RIAs) are a category of events required for research reactor safety analysis. A subset of this is unprotected RIAs, in which mechanical systems or human intervention are not credited in the response of the system.

MTR-type reactors are self-limiting up to a reactivity insertion limit beyond which fuel damage occurs. This characteristic was studied in the BORAX and SPERT full-scale reactor tests. This paper describes a parametric analysis of the experimental data and a methodology for determining these limits from this data set for any MTR-type reactor.

This approach was used in the recent McMaster Nuclear Reactor (MNR) Safety Analysis Report update. A conservative step reactivity insertion limit of 11 mk was determined for the MNR LEU Reference Core, based on an irradiated-fuel-blistering safety criterion. An associated stability limit of 21 mk was also estimated.

1. Introduction

Reactivity initiated accidents (RIAs) are a category of events required for research reactor safety analysis. A subset of this is unprotected RIAs, in which mechanical systems or human intervention are not credited in the response of the system.

MTR-type (*i.e.*, light-water cooled and moderated, plate fuel) reactors are strongly self-limiting up to a reactivity insertion limit beyond which fuel damage occurs. This characteristic was studied in the BORAX (Boiling Water Reactor Experiments) and SPERT (Special Power Excursion Reactor Tests) reactor tests of the 1950s and 1960s in the USA for HEU cores and was found to be effective, reliable, and highly predictable [1,2]. Low enrichment oxide cores were also studied which qualitatively demonstrate the additional effect of fuel temperature feedback [3]. Together, the BORAX-I and SPERT MTR-type cores represent a range of various system parameters including: core size, fuel plate spacing and loading, operating temperature, pressure, and coolant flow.

Power and temperature transients were studied for both step (*i.e.*, fast) and ramp (*i.e.*, slow) reactivity insertions of varying magnitudes including the range associated with fuel damage and up to the point of core disassembly. In terms of safety analysis, examples of fast reactivity insertion accidents are expulsion or fast removal of absorber rods, fast sample movement, or fuel drop during fuelling operations. Examples of slow reactivity insertion accidents are the start-up transient (uncontrolled motor withdrawal of absorber rods), slow sample movement, or a leaking irradiation vessel.

This paper presents a methodology for determining RIA limits for any MTR-type reactor from this experimental data. The safety criterion adopted in this study is the onset of fuel damage associated with a fuel cladding temperature. This is considered a safety limit since breaching the fuel plate cladding represents a compromise of the first level of containment for radiation release. Limits are found by determining the maximum reactivity insertion which does not achieve or exceed this temperature.

The approach presented herein uses correlations in the reactor test data accounting for differences in important system parameters. A semi-empirical approach is used to quantify parametric dependencies

on core size, power distribution, void coefficient, and initial degree of subcooling. An extension is also presented with respect to LEU fuel.

This approach provides an extension to PSA analysis of events with probabilities of occurrence of less than one in one million years (typical PSA cutoff for analysis). It also presents an alternative to simulation-based studies where quantitative accuracy is lacking due to modelling limitations [4]. These limitations appear mainly in transient boiling and hydraulic behaviour which limits the accuracy of such studies to that of the initial power pulse. The peak fuel temperatures occur in the post-power-burst stage of the transient and depend on hydraulic aspects of the reactor core. Insight is also provided into further validation and improved use of simulation tools which have been benchmarked against SPERT HEU data for the initial stage of the transient response.

This work further quantifies and extends previous use of experimental data in the context of research reactor safety analysis [5-9]. It has been incorporated in the most recent version of the McMaster Nuclear Reactor (MNR) Safety Analysis Report [10].

2. Transient Characteristics

A stylized self-limited power excursion for an HEU MTR-type reactor core is shown in Figure 1.

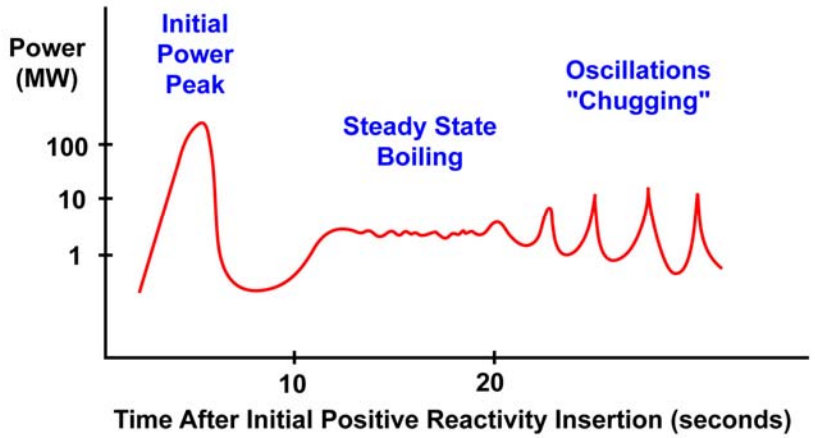

Figure 1: Self-Limited MTR-type Reactor Power Excursion

A convenient index of the transient is the reciprocal asymptotic or minimum reactor period of the initial power burst. For reactivity insertions in the range of interest (short period range), this period is on the order of 35 msec or shorter. It is found that for an HEU MTR-type system, power initially increases exponentially until feedback mechanisms can become effective. If these are fast and large enough the power increase is arrested, returning the system to a new equilibrium, or semi-stable state, which can involve steady-state coolant boiling, low amplitude power oscillations, or large amplitude power oscillations ("chugging") in which the coolant cyclically is expelled from and refills the core.

Ramp insertions of reactivity produce similar excursions to the step insertions of reactivity, but with a reduced, or absent initial power pulse. This reduction depends on the rate of reactivity insertion.

The wealth of data from the BORAX and SPERT reactor tests show that the self-limiting response of an MTR-type reactor is highly predictable and consistent for a wide range of system parameters such as plate spacing, fuel loading, and core size. This is illustrated in the correlated data plots of maximum power (P_{max}), energy generated to the time of maximum power (E_{tm}), and the maximum fuel plate surface temperature rise (ΔT_{max}) for the different test cores as functions of the transient reciprocal period (α_o). The parameters P_{max}, E_{tm}, and ΔT_{max} are all indicators of proximity and approach to the onset of fuel damage. The maximum power data for the BORAX-I and SPERT HEU test cores is shown in Figure 2.

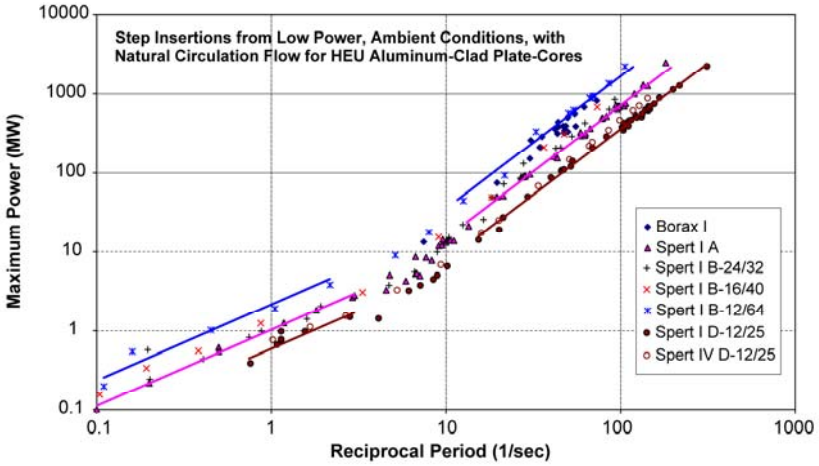

Figure 2: Peak Power Experimental Data

For an HEU MTR-type core the self-limiting response in the short period range is governed primarily by coolant voiding producing negative reactivity feedback [11]. In this sense the self-limiting response depends on the voiding characteristics of the core which in turn depend on nuclear characteristics (*e.g.*, void coefficient), heat transfer characteristics (*e.g.*, thermal resistance and heat transport) of fuel and coolant, and initial conditions of the system (*e.g.*, pressure, temperature). For LEU fuel the self-limiting behaviour is further strengthened by negative fuel temperature feedback.

Various degrees of fuel damage have been observed for periods less than 10 msec ($\alpha_o > 100$ sec^{-1}). These various types and degrees of fuel damage are directly tied to maximum fuel plate temperatures and progress in severity with shortening reactor period and increasing maximum temperature.

3. Data Analysis

3.1 Description of the Data

The step-insertion power and energy response of an HEU MTR-type core is described well by the simple lumped parameter analytical model [12,13]:

$$\frac{P'(t)}{P(t)} = \alpha_o - w\left[E\left(t - t_d\right)\right]^n \qquad (1)$$

Where $P(t)$ is the power at time t, $E(t\text{-}t_d)$ is the energy generated to time $(t\text{-}t_d)$, t_d is a delay time for thermal feedback, α_o is the reactor period, w is a shutdown reactivity coefficient, and n is the exponent of the energy dependence. The prime superscript indicates the derivative with respect to time. This is referred to as the Shutdown Model and provides the following expression for the peak power in the initial power burst:

$$P_{max} = \frac{\alpha_o^{(n+1)/n}}{w^{1/n}} e^{(\alpha_o t_d - 1/n)} \qquad (2)$$

The product $(\alpha_o t_d)$ is found to be approximately constant over the short period range of transients [14]. A similar expression is found for the energy generation to the time of peak power during a transient.

Curve fitting was performed on the P_{max}, E_{tm}, and ΔT_{max} *vs.* α_o data using the above expressions and an exponential function relating the maximum temperature change and the reciprocal period, *i.e.*,

$$\begin{aligned} P_{max} &= b_1\, \alpha_o^{\,m_1} \\ E_{tm} &= b_2\, \alpha_o^{\,m_2} \\ \Delta T_{max} &= b_3\, e^{\alpha_o m_3} \end{aligned} \tag{3}$$

The uncertainties in the test data have been conservatively estimated at 5% for the power, energy and temperature measurements and 10% for the period from information in the original technical reports. Details of this assessment are found in Reference [15].

3.2 Variation with Core Size

It is found that differences in different sets of the test data can be expressed in terms of differences in the system feedback parameter. The trends in the power and energy data are found to be consistent in the maximum temperature change data when the power and energy are related to the maximum temperature change in terms of peak power and energy density, *i.e.*,

$$\begin{aligned} \Delta T_{max} &\propto P_{max}/V_f \times PPF \\ &\propto E_{tm}/V_f \times PPF \end{aligned} \tag{4}$$

V_f is the fuel meat volume of the core, and PPF is the overall power peaking factor. This relation allows transformations applied to power and energy data to be similarly applied to temperature test data provided core size and power distribution differences are taken into account.

3.3 Variation with Void Coefficient

The test data from ambient initial temperature conditions was correlated to a shutdown coefficient expressed in terms of the uniform void coefficient of the core and the average channel volume for each test core. It takes the form:

$$w = K_c \left(\frac{-C_{void}\, V_c}{\ell} \right) \tag{5}$$

w is the shutdown coefficient in equation (1), K_c is a constant of proportionality, C_{void} is the uniform void coefficient of reactivity (in reactivity per unit void volume), V_c is the volume of a representative coolant channel within the void distribution, and ℓ is the prompt neutron lifetime. This relation was derived heuristically, based on the concept of boundary layer voiding of the coolant, fast full-channel expansion of the steam to force the remaining coolant from the core, and uniform core voiding. It differs from earlier work based on only part of the data set which did not include the volume component [16] and was found to not be suitable for the entire set of test cores. The scaling then takes the form:

$$\begin{aligned} P_{max,j} &= \left(\frac{w_j}{w_i} \right)^v P_{max,i} \\ v &= 0.726 \pm 0.063 \end{aligned} \tag{6}$$

The parameter v has been found empirically from fitting the test data. The power test data is shown in Figure 3 both before and after scaling with the void-shutdown coefficient.

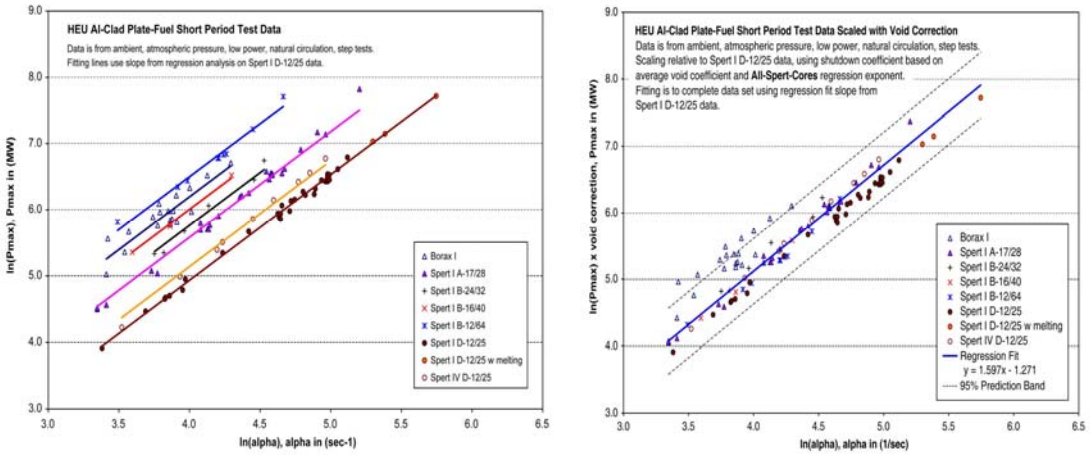

Figure 3: Power Test Data Before and After Scaling with the Void-Shutdown Coefficient

This scaling was performed using measured void coefficients for the SPERT cores and a simulation-based value for the BORAX-I core. Values of V_c and ℓ were taken from the literature and are summarized in Reference [15]. The same scaling is applicable to the energy and temperature data provided the latter is also scaled to core size and power distribution.

3.4 Variation with Subcooling

Subcooling is defined as the difference in temperature between the saturation temperature of the coolant and the actual temperature of the coolant, *i.e.*,

$$T_{sub} \equiv T_{saturation}^{coolant} - T_{initial}^{coolant} \tag{7}$$

A larger degree of subcooling means a lower initial coolant temperature. As subcooling is increased more energy must be transferred from the fuel to the coolant, translating into a longer delay time before the self-limiting void feedback can take effect. The result is larger energy generation, peak power, and fuel plate temperature rises. The BORAX-I subcooling test data were correlated and provide a relation between change in subcooling and change in maximum temperature rise:

$$\Delta T_{max}\left(T_{sub,i}\right) = \frac{(1+s\times T_{sub,i})}{(1+s\times T_{sub,j})} \times \Delta T_{max}\left(T_{sub,j}\right) \tag{8}$$

$$s = 0.0424 \pm 0.0071 \quad /^{\circ}C$$

This relation is consistent with trends observed in the SPERT subcooling test series and is an extension to work previously reported on the BORAX-I data [17].

3.5 Variation with Doppler Coefficient

As demonstrated by the tests on LEU oxide rod fuel as part of the SPERT Project the large magnitude and prompt in nature Doppler feedback associated with LEU fuel provides a second major contribution to the self-limiting nature of a reactor core. This characteristic has been studied previously using the PARET kinetics code and the IAEA 10MW Benchmark Reactor problem [4,18]. The ratio of limiting step insertion of reactivity from these simulation results is found to be 1.18 for an instantaneous reactivity insertion, increasing significantly to 2.29 when the duration of the reactivity insertion is lengthened to 0.5 seconds. This provides a first estimate for an extension of the HEU experimental data to LEU fuel.

4. Reactivity Limits

The resulting methodology incorporates the parametric dependencies outlined above. This involves scaling the experimental test data to account for differences in system parameters between the test cores and a generic MTR-type core of interest. The methodology is based on relations found from the step-insertion test data but can be applied to both ramp-insertions of reactivity and also to the longer-term stability limits for the system based on equivalence arguments. Stability limits can be found by the additional credit of the temperature defect from initial conditions to those associated with steady state boiling. Ramp insertion limits can be found by equating the minimum period produced in the ramp-initiated transient to the step-insertion asymptotic period. The steps in the methodology are as follows:

- Start with BORAX/SPERT ΔT_{max} *vs.* α_o test data
- Scale for difference in subcooling
- Scale for difference in core size
- Scale for difference in power peaking
- Scale for difference in void coefficient
- Convert limiting period to limiting reactivity
- Scale for application to LEU fuel
- Adjust to associated ramp insertion or stability limit

Mathematically the HEU data scaling is expressed as:

$$\Delta T_{max}^{TC} = \Delta T_{max}^{i} \times \frac{V_f^i}{V_f^{TC}} \times \frac{PPF^{TC}}{PPF^i} \times \left(\frac{w^i}{w^{TC}} \right)^v \times \frac{(1 + s \times T_{sub}^{TC})}{(1 + s \times T_{sub}^{i})} \qquad (9)$$

The superscripts *TC* and *i* refer to the test core and the system of interest respectively. For stability limits the system of interest temperature coefficient of reactivity is required while for application to ramp-reactivity insertions the equivalence relationship is needed. Delayed neutron characteristics are also required to convert period to reactivity. The entire methodology may also be applied in reverse to determine maximum power, energy generation to peak power and maximum fuel temperature rise from limiting reactivity values.

This analysis approach was used in the recent MNR Safety Analysis Report update [10]. A conservative step reactivity insertion limit of 11 mk was determined for the MNR LEU Reference Core, based on an irradiated-fuel-blistering safety criterion. An associated stability limit of 21 mk was also estimated. The data scaling and associated system conditions have at all times been kept conservative in the analysis to account for both uncertainties in the test data and in the statistics and empirical parameter factors.

5. Conclusions

A quantitative methodology for determining RIA limits for unprotected transients from the HEU experimental data has been developed. For HEU fuel the primary parameters are found to be core size, power distribution, channel-volume-based void reactivity feedback, and initial subcooling of the reactor. Extensions to LEU fuel are included and based on existing simulation results.

Step insertion and stability reactivity limits are estimated for the MNR LEU Reference Core as 11 mk and 21 mk respectively and has been incorporated into the MNR safety case. Further details of the analysis can be found in Reference [15].

This analysis approach provides extensions to PSA methods for rare events and an alternative to simulation-based studies which are limited in their accuracy. Information gained via this study is also valuable in conjunction with simulation work.

6. References

[1] J. R. Dietrich, D. C. Layman, "Transient and Steady State Characteristics of a Boiling Reactor. The Borax Experiments, 1953", ANL-5211 (also listed as AECD-3840), Argonne National Laboratory, USA, February 1954.

[2] W. E. Nyer, S. G. Forbes, F. L. Bentzen, G. O. Bright, F. Schroeder, T. R. Wilson, "Experimental Investigations of Reactor Transients", US AEC Technical Report IDO-16285, Phillips Petroleum Co., April 20, 1956.

[3] A. H. Spano, J. E. Barry, L. A. Stephan, J. C. Young, "Self-Limiting Power Excursion Tests of a Water-Moderated Low-Enrichment UO_2 Core in Spert I", US AEC Technical Report IDO-16751, Phillips Petroleum Co., February 28, 1962.

[4] W. L. Woodruff, "A Kinetics and Thermal-Hydraulics Capability for the Analysis of Research Reactors", Nuclear Technology, v.64, February 1984, pp. 196-206.

[5] Ford Nuclear Reactor - Description and Operation, Michigan Memorial Phoenix Project, University of Michigan, June 1957.

[6] Safety Analysis, Ford Nuclear Reactor, Michigan Memorial Project, University of Michigan, Docket 50-2, License R-28, 1984.

[7] Safety Analysis Report for the MIT Research Reactor (MITR-II), MITNE-115, October 1970.

[8] Safety Analysis Report for the MIT Research Reactor, draft version of Chapter 13, *circa* November 2002.

[9] McMaster Nuclear Reactor Safety Analysis Report, McMaster University, Hamilton, Ontario, Canada, 1972.

[10] McMaster Nuclear Reactor Safety Analysis Report, McMaster University, Hamilton, Ontario, Canada, February 2002.

[11] J. C. Haire, Editor, "Quarterly Technical Report - Spert Project - April, May, June, 1959", US AEC Technical Report IDO-16584, Phillips Petroleum Co., April 12, 1960.

[12] S. G. Forbes, F. L. Bentzen, P. French, J. E. Grund, J. C. Haire, W. E. Nyer, R. F. Walker, "Analysis of Self-Shutdown Behavior in the Spert I Reactor", US AEC Technical Report IDO-16528, Phillips Petroleum Co., July 23, 1959.

[13] T. J. Thompson, J. G. Beckerly, editors, The Technology of Nuclear Reactor Safety, Vol. 1, "Reactor Physics and Control", Chapter 7, W. E. Nyer, "Mathematical Models of Fast Transients", The MIT Press, 1964.

[14] G.O. Bright, editor, "Quarterly Progress Report - January, February, March, 1958 - Reactor Projects Branch", US AEC Technical Report IDO-16452, Phillips Petroleum Co., September 10, 1958.

[15] S.E. Day, The Use of Experimental Data in an MTR-Type Nuclear Reactor Safety Analysis, PhD Thesis, McMaster University, Hamilton, Ontario, Canada, February 2006.

[16] T.J. Thompson, J.G. Beckerly, editors, The Technology of Nuclear Reactor Safety, Vol. 1, "Reactor Physics and Control", Chapter 8, J.A. Thie, "Water Reactor Kinetics", The MIT Press, 1964.

[17] W. K. Luckow, L. C. Widdoes, "Predicting Reactor Temperature Excursions by Extrapolating Borax Data", Nucleonics, v. 14, n. 1, pp. 23-25, January 1956.

[18] J. E. Matos, E. M. Pennington, K. E. Freese, W. L. Woodruff, "Safety-Related Benchmark Calculations for MTR-Type Reactors with HEU, MEU and LEU Fuels", ANL, IAEA-TECDOC-643, v.3, Appendix G-1, 1992.

SAFETY ANALYSIS OF RESEARCH REACTORS WITH BEST ESTIMATE COMPUTATIONAL TOOLS

M. ADORNI, A. BOUSBIA-SALAH and F. D'AURIA
DIMNP - University of Pisa
2 Via Diotisalvi, 56126 Pisa - Italy

and

R. NABBI
Central Research Reactor Division, Forschungszentrum Jülich
52425 Jülich - Germany

ABSTRACT

Best Estimate computer codes have been, so far, developed for safety analysis of nuclear power plants and were extensively validated against a large set of separate effects and integral test facilities experimental data relevant to such kind of reactors. With the sustained development in computer technology, the possibilities of code capabilities have been enlarged substantially. Consequently, advanced safety evaluations and design optimizations that were not possible a few years ago can now be performed. According to the IAEA Research Reactor Database (RRDB) 651 research reactors have been constructed around the world for civilian applications. On the basis of the RRDB, 284 research reactors are currently in operation, 258 are shut down and 109 have been decommissioned. The purpose of the present paper is to provide an overview of the accident analysis technology applied to the research reactor, with emphasis given to the capabilities of computational tools.

1. Introduction

An established international expertise in relation to computational tools, procedures for their application including best-estimate methods supported by uncertainty evaluation and comprehensive experimental database exists within the safety technology of NPP. The importance of transferring NPP safety technology tools and methods to research reactor (RR) safety technology has been noted in recent IAEA activities. However, the ranges of parameters of interest to RR are different from those for NPP: this is namely true for fuel composition, system pressure, adopted materials and overall system geometric configuration. The large variety of research reactors prevented so far the achievement of systematic and detailed lists of initiating events based upon qualified PSA (Probabilistic Safety Assessment) studies with results endorsed by the international community. However, bounding and generalized lists of events are available from IAEA documents and can be considered for deeper studies in the area.

An established technology exists for development, qualification and application of system thermal hydraulics codes suitable to be adopted for accident analysis in research reactors. This derives from NPP technology. The applicability of system codes like RELAP5, COBRA and MARS to the research reactor needs has been confirmed from recent IAEA. Definitely, system codes are mature for application to transient analysis in research reactors. However, code limitations have been found in predicting pressure drops as a function of mass flux at low values of mass flux when nucleate boiling occurs. The importance of the Whittle & Forgan experiments shall be mentioned, as well as the dependence of results from the nodding (cell subdivision) adopted by the code users. Several code user choices, including time step may have a significant effect upon prediction, thus confirming the need for detailed code user guidelines. Furthermore, code validation must be demonstrated for the range of parameters of interest to research reactors.

The crucial role of uncertainty in research reactor technology has been emphasized, a) for the design, with main reference to the prediction of the nominal steady-state conditions and, b) for the safety, with main reference to the prediction of the time evolution of significant safety parameters. It has been found that suitable-mature methods exist, but the spread of these methods and procedures within the community of scientists working in research reactor technology is limited.

2. Topics of interest for accident analysis in RR and current status

A list of topics relevant to the deterministic accident analysis in research reactors is provided below.
- *Postulated Initiating Events*. The identification of accident scenarios, typically derived by considering probability of occurrences and severity of consequences, constitutes the first step needed for performing deterministic safety analyses.
- *Acceptance criteria*. The availability of 'thresholds of acceptability' for consequences of accident, as a function of the probability of occurrence of the event, constitute the second requirement for deterministic safety analyses: namely results of the analyses shall be compared with 'limiting values'. Acceptance criteria are imposed by national authorities and are not connected with the deterministic safety analysis.
- *Experimental database*. Computational tools are used to perform deterministic analyses (see below) and experimental data are needed to demonstrate the quality of those tools. Experimental data can also be used directly to improve the design and the performance of research reactors.
- *Qualification of system codes*. System codes, widely used within the safety technology of Nuclear Power Plants (NPP), can be used for the deterministic analysis of accidents in Research Reactors (RR). The application must be based upon the evaluation of the complexity of the transient: in a number of cases owing to the 'simple' configuration of RR compared with NPP, simpler tools including analytical-hand calculations should be used. However, for the cases when system codes are needed, proper demonstrations of qualification must be provided.
- *Uncertainty in research reactor technology*. The role of uncertainty has been considered at two levels: a) design of research reactors, mostly addressed to the calculation of nominal steady state operating conditions, and b) evaluating the results from best-estimated predictions performed by thermal-hydraulic system codes, mostly addressed to the calculation of transient scenarios. Origins and impacts of uncertainty within both the frameworks are discussed in [1]. Methods and procedures to deal with uncertainty are presented in the same reference.

3. Example from Code Qualification Process

With widespread use of research reactor, there is a real need to get more realistic simulations of the phenomena involved during steady state and transient conditions, and eventually the identification of design/safety requirements that can be relaxed or enhanced. Several attempts were performed to assess the applicability of Best Estimate codes to RR operating conditions [2]. Relevant assessments were applied against the following cases.

4. The IAEA 10 MW Benchmark Problem

The IAEA Benchmark is based upon one of the SPERT series test reactors. A standard-quality RELAP5 nodalization has been developed and applied [2], [3] (Figs 1, 2). The reactor pool above the core zone is modelled in order to adequately simulate the natural convection process. The benchmark problem consists in analysing 'controlled' (or 'protected) transients in MTR Highly Enriched Uranium core (HEU) and Low Enriched Uranium (LEU) cores. The boundary conditions for the analysis are demanding from the thermal-hydraulic point of view. The Natural Convection Valve (NCV), as modelled in the RELAP5 nodalization, allows a flow reversal and the establishment of passive decay heat removal process by natural circulation flow.

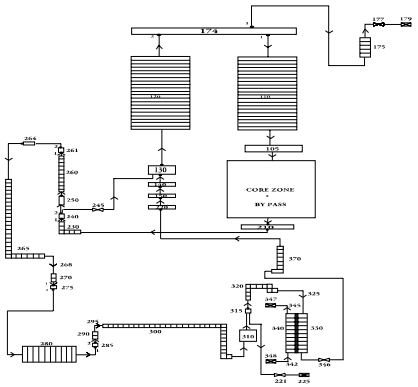

Fig 1 Nodalization for RELAP5

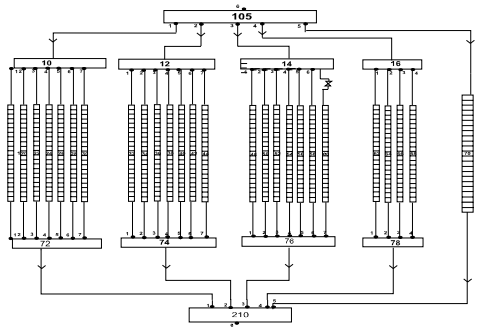

Fig 2 RELAP5 Core Nodalization

The Fast RIA (FRIA) transients are initiated by a super prompt ramp positive reactivity addition of \$1.5/0.5 s in the HEU and LEU cores. The Slow RIA (SRIA) consists in a continuous insertion of 9¢ /s in the HEU core and 10 ¢/s in the LEU core. The reactor is assumed to be at an initial operating power of 1W and with full downward cooling flow (not as the benchmark specifications which consider initial upward flow). The safety system is activated when the core power exceeds 12 MW, by inducing a negative reactivity of -\$10 in 0.5 sec within a response delay time of 0.025 s. The flow decay is modelled as an exponential (exp(-t/T)) decrease with a period T equal to 1 s and 25 s for the Fast LOFA (FLOFA) and the Slow LOFA (SLOFA) case, respectively. The LOFA transients are initiated at a nominal core power of 12 MW and full core downward cooling flow conditions. The reactor scrams when the flow decay is reduced by 15%, with a response delay time of 0.2 s. Representative results are given in Figs. 3 to 6, where comparison is made, when applicable, with reference results obtained by the RR devoted codes PARET and RETRAC.

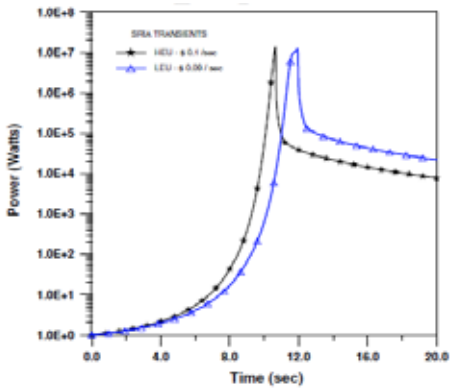

Fig 3. Core power during SRIA

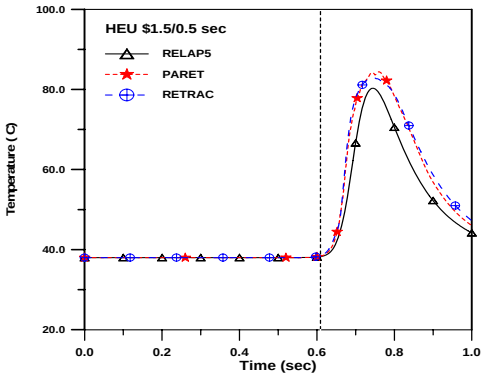

Fig 4. Outlet fluid temperature during

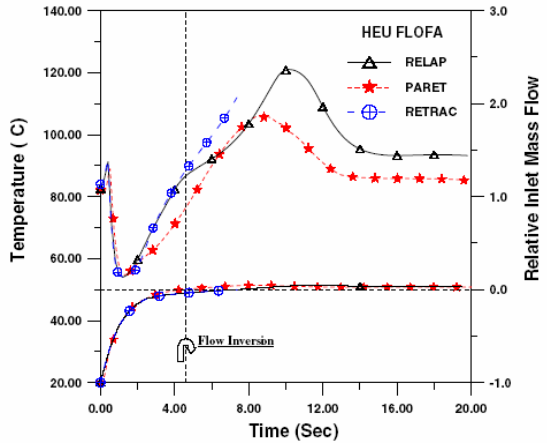

Fig 5. Clad surface temperature and relative mass flow rate during SLOFA transient

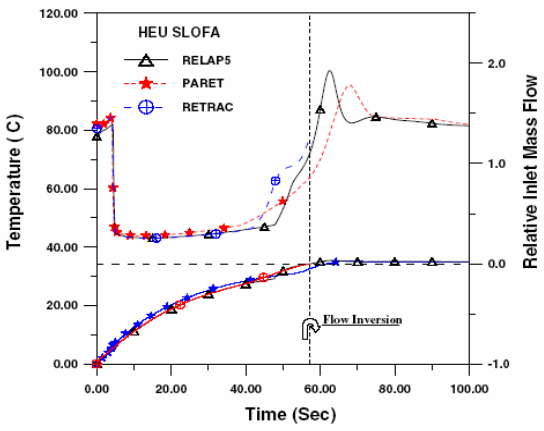

Fig 6. Clad surface temperature and relative inlet mass flow rate during FLOFA

Relevant experimental data (Whittle & Forgan experiments) and Relap5 calculation results for typical RR conditions are compared in Fig. 7, [4].

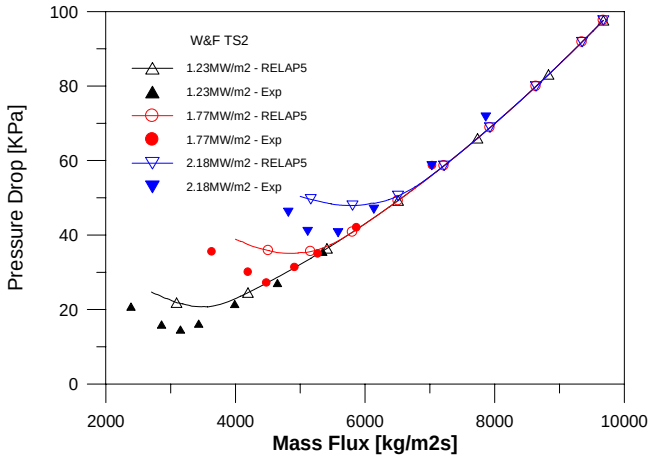

Fig 7. Pressure Drop Characteristic curve for W&F TS2

5. FRJ 2 Research Reactor

The Relap5 code has been applied to the safety evaluation of the FRJ2, 23 MW RR, installed at Juelich research centre. A global view of the reactor is given in Fig 8 [5]. The 'oblique' Control Rods (CR) can be observed: in case of 'free' CR drop, a negative insertion of reactivity is followed by a reactivity increase (Fig 9).

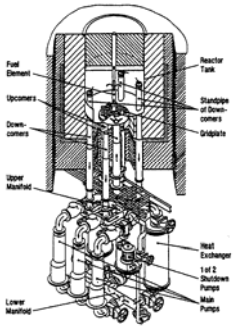

Fig 8. Global view of the cooling system of the FRJ-2

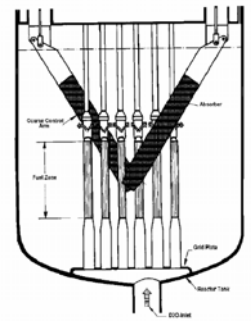

Fig 9. FRJ-2 core and CCA arrangement inside the reactor tank

A detailed Relap5 nodalisation, based on CATHENA one, has been developed including more than 500 hydraulic nodes and about 4000 meshes for conduction heat transfer, Figs 10 to 12. The considered transient is a CR drop without scram originated in the complex geometry of FRJ2 reactor. A result of the analysis by RELAP5 and CATHENA code of the RIA w/o scram in the FRJ2 reactor is given in Fig 13.

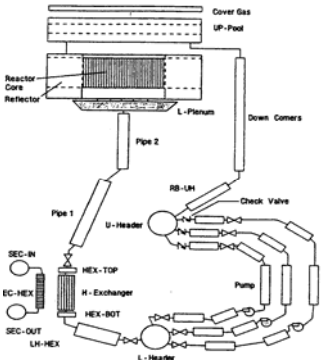

Fig 10. Nodalization for CATHENA

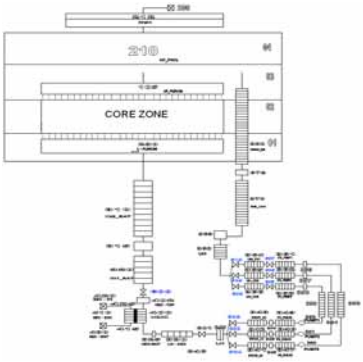

Fig 11. Nodalization for RELAP5

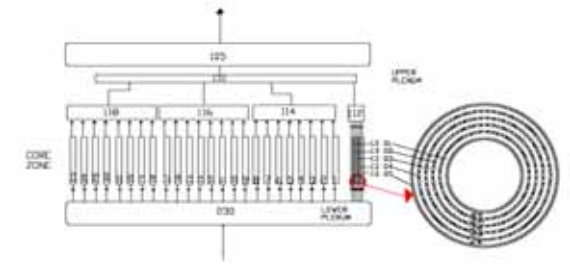

Fig 12 RELAP5 Core Nodalization

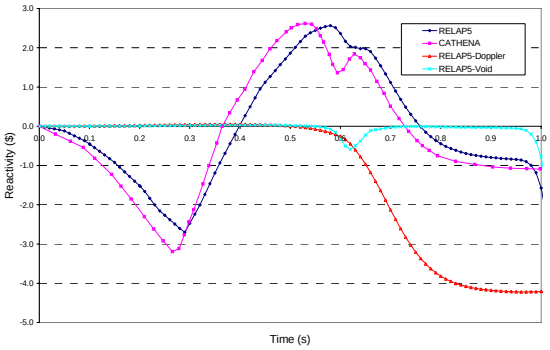

Fig 13 Core Reactivity

6. Conclusion

The demonstration of applicability of qualified best-estimate system codes to RR accident analysis constitutes the key message from this paper: a proper accident analysis technology should be developed for RR that could benefit of the experience available from NPP, considering that the risk level and the cost associated with RR are orders of magnitude lower. Recommendations are provided hereafter distinguishing between potential RR system thermal-hydraulic code users and decision makers in the area.

Recommendations to the users of computational tools are:

- To consider experimental data and to perform code-to-experiment comparison before any code application to prediction relevant to the RR design or safety analysis.
- To demonstrate that any code adopted for design and safety is qualified.
- To consider that any best-estimate code, even though supported by the use of the optimised procedures, produces results that are affected by an unknown error, i.e. uncertainty.

Recommendations to decision makers focus on establishing an international understanding in the area:

- To plan "benchmark" exercises in conditions where neutron kinetics and natural circulation are relevant.
- To promote the use of PSA techniques, establishing detailed PIE (postulated initiating events) lists.
- To make an effort to establish 'validation-matrices' for computational tools.
- To plan suitable training in the area of RR accident analysis.
- To consider innovative techniques including of CFD (Computational Fluid Dynamics) and coupled three-dimensional neutron kinetics codes and thermal-hydraulic system codes.

7. References

[1] IAEA *"Uncertainty Evaluation in Best Estimate Safety Analysis for Nuclear Power Plants"* IAEA report, to be issued.

[2] T. Hamidouche, A. Bousbia-Salah, M. Adorni, F. D'Auria, "*Dynamic Calculations of the IAEA Safety MTR Research Reactor Benchmark Problem using RELAP5/3.2 Code*". Annals of Nuclear Energy, 31, pages 1385-1402. 2004.

[3] B. Di Maro, F. Pierro, M. Adorni, A. Bousbia-Salah, D'Auria, *"Safety analysis of loss of flow transients in a typical research reactor by RELAP5/MOD3.3"*, Proc. Int. Conference "Nuclear Energy for New Europe 2003", Portorož (Slovenia), September 8-11, 2003.

[4] Tewfik Hamidouche and Anis Bousbia-salah RELAP5/3.2 "*Assessment against low pressure onset of flow instability in parallel heated channels*" Annals of Nuclear Energy Volume 33, Issue 6 , April 2006, Pages 510-520.

[5] M. Adorni, A. Bousbia-Salah, D'Auria F., Nabbi R., *"Application of best estimate thermal-hydraulic codes for the safety analysis of research reactors"* 10th Int. Top. Meet. on Research Reactor fuel management, April 30 – May 3, 2006, Sofia (Bulgaria).

KINETIC PARAMETERS CALCULATION AND MEASUREMENTS DURING THE OPAL COMMISSIONING

DANIEL F. HERGENREDER, CARLOS A. LECOT AND EDUARDO A. VILLARINO

INVAP S.E., Nuclear Projects Department, Nuclear Engineering Division
F.P. Moreno 1089

(R8400AMU) S.C. de Bariloche, Río Negro, Argentina

ABSTRACT

During the Commissioning Stage of the OPAL Research Reactor (Australia) the Prompt Neutron Decay constant was measured by analysing the inherent fluctuations that occur in the neutron population. The ratio of the variance to the mean number of counts as a function of counting time is used to determine the α parameter. This technique is also called Feynman-α Method.
The CITVAP and MCNP codes were used to calculate the prompt neutron decay constant for the first core configuration. By means of two different MCNP calculations, one considering prompt fission neutrons only and another with total fission neutrons; the effective delayed neutron fraction is estimated.
The experimental method, the measured value as well as the numerical assessment are presented in this paper. A good agreement was obtained between measurements and calculations and a comparison is presented in the paper.

1. Introduction

The OPAL Research Reactor is a multi-purpose open-pool type reactor. The nominal fission power of the reactor is 20 MW. The core is located inside a chimney, surrounded by heavy water contained in the Reflector Vessel. The whole assembly is at the bottom of the Reactor Pool, which is full of de-mineralized light water acting as coolant and moderator and biological shielding.

Several irradiation facilities are located around the reactor core. Three types of neutron sources: a cold neutron source with two tangential beams and several neutron guides, a thermal neutron source with two beams and several neutron guides, and a space reserved for a future hot neutron source with a beam.

During the design stage, core calculations were performed to obtain the effective delayed neutron fraction (β_{eff}), the neutron lifetime (Λ) and its ratio, the prompt neutron decay constant (α), which is used in the Safety Analysis Report.

The CONDOR - CITVAP codes (references [1] and [2]) and MCNP code (reference [3]) were used to calculate the prompt neutron decay constant for the first core configuration.

Both the delayed neutron fraction and the neutron lifetime were assessed with the CITVAP code using microscopic cross-section libraries.
Carrying out an MCNP calculation with an external neutron source allows the estimation of the core neutron population as a function of time. Through the analysis of the neutron population, the prompt neutron decay constant (α) is obtained.

The effective delayed neutron fraction is estimated by means of two different MCNP calculations, one considering prompt fission neutrons only and another one with total fission neutrons.

2. Description of the calculation lines

There are two calculation lines used to estimate the kinetic parameters. The calculation lines are the CONDOR – CITVAP line and the MCNP line.

2.1. CONDOR - CITVAP calculation line

The CONDOR code for neutronic calculations is used to calculate fuel cells, fuel-rod clusters, as well as fuel plates with slab geometry or 2D geometry. Flux distribution within the region of interest is obtained through the collision probability method or the Heterogeneous Response Method in a multi-group scheme with various types of boundary conditions.
The CITVAP code used to carry out the core design of the OPAL reactor is a new version of the CITATION-II code, developed by INVAP's Nuclear Engineering Division. The code was developed to improve CITATION-II performance. In addition, programming modifications were performed for its implementation on personal computers.
The code solves 1, 2 or 3-dimensional multi-group diffusion equations in rectangular or cylindrical geometry. Spatial discretization can also be achieved with triangular or hexagonal meshes. Nuclear data can be provided as microscopic or macroscopic cross section libraries.
CITVAP performs flux and adjoint flux calculations in order to assess the prompt neutron lifetime and delayed neutron fraction. Energy spectra with a higher number of energy groups (especially in the fast group region) are used to take into account the difference between the delayed and prompt neutrons.

2.2. MCNP calculation line

The MCNP code is a well knows Monte Carlo code that was used to design the irradiation facilities and to verify some neutron parameters through an independent calculation method. This is a Monte Carlo transport code for neutron and gamma calculations using ENDF/B-VI cross sections in any order and performs 3-D calculations.

3. Kinetic Parameters Calculation using MCNP

The effective delayed neutron fraction was calculated with MCNP under the following considerations:
The nuclear delayed fraction is the ratio between the delayed neutrons and the total neutron generated by fission, that is:

$$\beta = \frac{\upsilon_d}{\upsilon_t} \qquad [1]$$

To obtain the effective delayed fraction is necessary to weight the delayed and total neutron fractions by the number of neutrons that can be produced in the next generation.

$$\beta_{eff} = \frac{\upsilon_d N_d}{\upsilon_t N_t} \qquad [2]$$

Where N_d is the number of neutrons that will be produced in the next generation by each delayed neutron.

$$N_d = \frac{\nu_t FR_d}{\nu_d} \qquad [3]$$

And N_t is the number of neutrons that will be produced in the next generation by each total neutron

$$N_t = \frac{\nu_t FR_t}{\nu_t} \qquad [4]$$

FR_d and FR_t are the fission rate produced by delayed neutron and total neutrons, respectively.
Replacing N_d and N_t in equation [2], the expression for β_{eff} is obtained.

$$\beta_{eff} = \frac{FR_d}{FR_t} \qquad [5]$$

This equation [5] is also presented in reference [4].

The β_{eff} was also calculated as the difference in the core reactivity when total neutrons are used and when only prompt neutrons is used.

To calculate the prompt neutron decay constant with MCNP it was simulated the Rossi-α experiment, reference [5]. A full detail model of the core and reflector vessel was used to carry out the calculations with an external neutron source. The neutron population in the core (meat material) as a function of time was analysed. The prompt neutron decay constant (α) is obtained fitting the neutron population as a function of time with an exponential function.
From the α parameter and the core reactivity, the neutron lifetime can be obtained.

4. Prompt Neutron Decay Constant Measurement

During the OPAL commissioning, the α constant was measured by analysing the inherent fluctuations that occur in the neutron population. The ratio of the variance to the mean number of counts as a function of counting time is used to determine de α parameter. This technique is also called Feynman-α Method, reference [6].
According to reference [6], the equation [6] relates the variance to mean ratio V(t) with the α parameter:

$$V(t) = \frac{N\sum_{i=1}^{N} C_i^2 - \left(\sum_{i=1}^{N} C_i\right)^2}{N\sum_{i=1}^{N} C_i} = 1 + \frac{\varepsilon\chi}{(\beta_{eff} - \rho)^2}\left[1 - \frac{(1 - e^{-\alpha t})}{\alpha t}\right] \qquad [6]$$

Where:
N: number of time intervals of length t analysed.
C_i: number of counts recorded during the time interval i of length t.
ε: absolute detector efficiency [Counts/Fission].
$\chi = \frac{\overline{\nu(\nu-1)}}{\overline{\nu}^2}$, where ν is the number of neutrons released during the fission. For the thermal fission of the Uranium-235 χ=0.795.
β_{eff}: effective delayed neutron fraction.
ρ: core reactivity.
α: prompt neutron decay constant, $\alpha = \frac{\beta_{eff} - \rho}{\Lambda}$. When the reactor is critical, $\alpha = \frac{\beta_{eff}}{\Lambda}$.
Λ: neutron lifetime.

To obtain α, the counting of a Fission Counter (FC) detector placed in the core is recorded in files for different core reactivities (all of them lower than zero). The information recorded in each file is the time interval between two successive counts.

The recorded file is analysed numerically. The software divide the measuring time in time intervals of length t and obtain the number of counts (C) recorded during each time interval (i) of length t. For that time interval of length t, V(t) is evaluated as the left side of equation [6].
V(t) is evaluated for different time length from 50 μs to 0.05 s with steps of 50 μs, that is, there are 1000 evaluations of the variance to mean ratio.
Figure 1 shows the variance to mean ratio V(t) for different core reactivities.

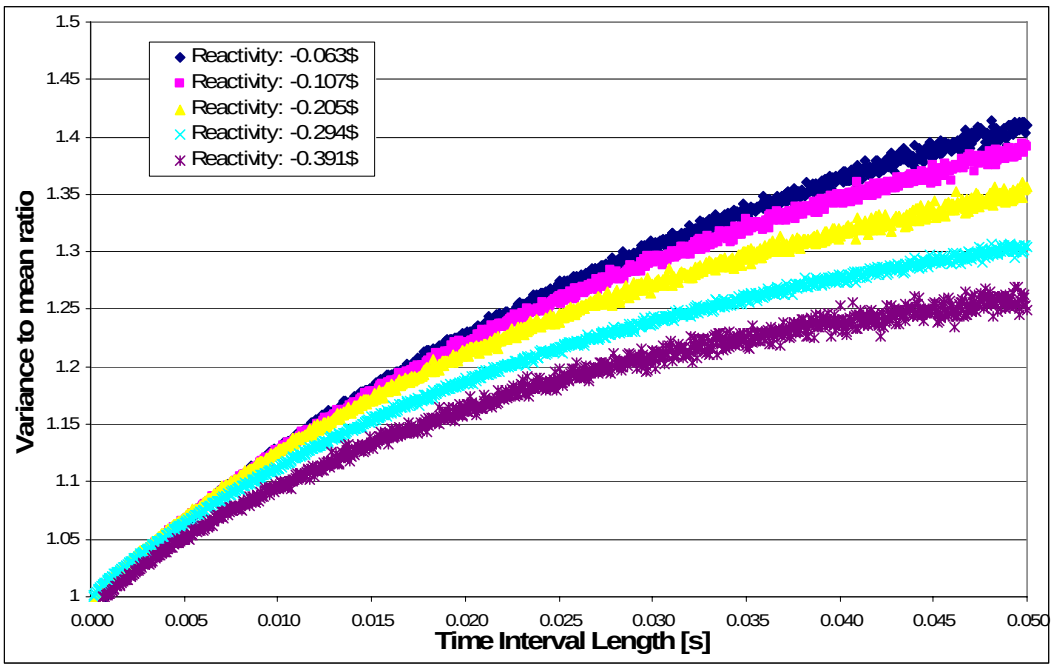

Figure 1: V(t) when the time interval length vary from 50 μs to 0.05 s with steps of 50 μs.

By fitting V(t) with the right side of equation [6] it is possible to obtain α for that core reactivity.
By repeating the FC counts recording process for different core reactivities the plot of α as a function of the core reactivity (ρ) is obtained, as shown in Figure 2.
The plot of α as function of the core reactivity (ρ) is adjusted by a linear fitting and the value of α when ρ=0 is β_{eff}/Λ.
For accurate experimental results it is essential that the detector efficiency ε be as high as possible, reference [7].

5. Results

The kinetic parameters of the OPAL Research Reactor were calculated with CITVAP and MCNP for the full core configuration, i.e., 16 Fuel Assemblies (FA).
Table 1 shows the calculated parameters β_{eff} and Λ for the 16 FA core.

	CITVAP	MCNP
β_{eff} [pcm]	768	769.5
Λ [μs]	171	171.6
α [1/s]	44.9	44.8

Table 1: β_{eff} and Λ for the first 16 FA core.

The β_{eff} for the first 16 FA core was also calculated by MCNP as the difference in the core reactivity when total neutrons are used and when only prompt neutrons given a value of 769.6 pcm.

Due to the fact that the measurements of kinetic parameters require high absolute detector efficiency, during the Commissioning of the OPAL reactor, the neutron decay constant was measured for the 15 FA core configuration, replacing one central FA by an FC detector.

To measure the α parameter, the Feynman-α method was used. The α parameter value was measured for different subcritical levels. The α(ρ) function was adjusted by a linear fitting and the value of α when ρ=0, i.e., the β_{eff}/Λ value, was obtained.

This experiment was also compared with the results obtained with MCNP simulating the Rossi-α experiment. The α parameter was obtained for different subcritical levels and adjusted by a linear fitting.
Figure 2 shows the comparison between measured and calculated values. From this figure it is worth noticing that the measured value for the α parameter, when ρ=0, is 38.1 1/s while the calculated value is 37.2 1/s.

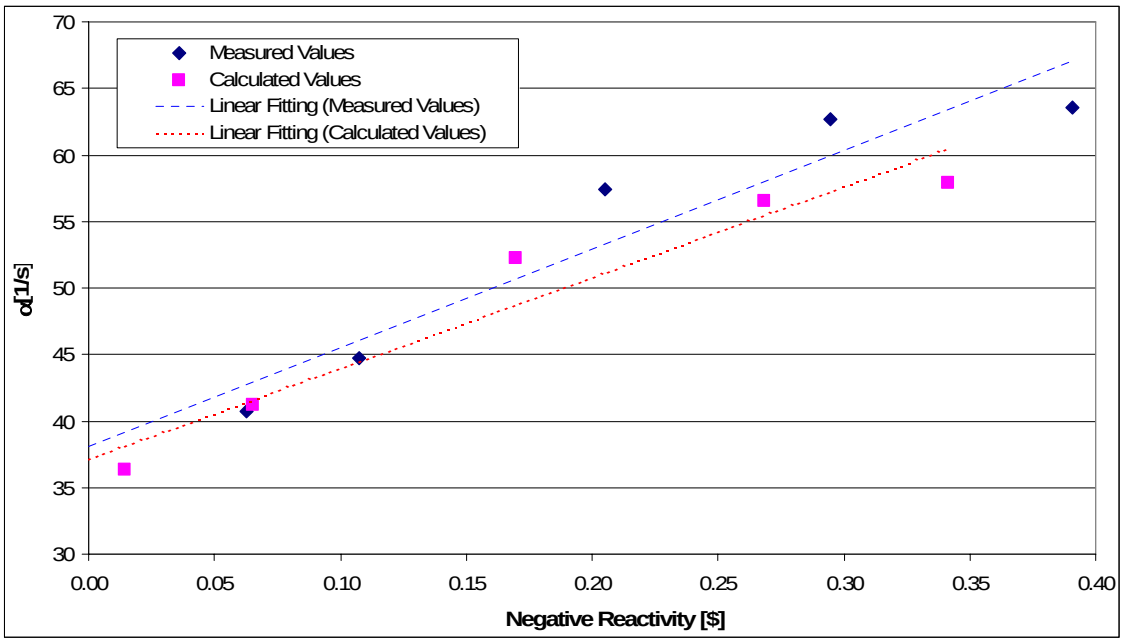

Figure 2: Parameter α as function of the core reactivity.

6. Conclusions

The MCNP code was used to obtain the kinetic parameters β_{eff} and Λ. There is a good agreement between the MCNP calculated values and the values obtained by the traditional calculation line for this parameters (CITVAP code).
The α parameter was measured with the Feynman-α method using the plant instrumentation (Fission Counter detector). There was good agreement between the measured α value and the MCNP calculated value following the Rossi-α experiment.

7. References

[1]. CONDOR Calculation Package, International Conference on the New Frontiers of Nuclear Technology : Reactor Physics, Safety and High-Performance Computing. Physor 2002
[2]. Eduardo Villarino and Carlos Lecot, **Neutronic calculation code CITVAP 3.1**. IX Encontro Nacional de Fisica de reatores e Termo-hidrualica. Caxambu. Brasil. October 1993.
[3]. Briesmeister, J. F., Ed., **MCNP - A General Monte Carlo N-Particle Transport Code, Version 4C,** LA13709-M, Los Alamos National Laboratory (April 2000).
[4]. Steven C. Van der Marck et al, **Calculating the effective delayed neutron fraction using Monte Carlo Techniques**, PHYSOR 2004, April 25-29, 2004.
[5]. G.S. Brunson et al, **Measuring the Prompt Period of a Reactor**, Nucleonics, Vol.15, N° 11 November, 1957.
[6]. IAEA Technical Report Series 138, **Kinetics and Noise Analysis of Zero-Power Reactors**, 1972.
[7]. WILLIAMS M.M.R., **Random Process in Nuclear Reactors**, First Edition 1974.

DETERMINATION OF SAFARI-1 NEUTRON FLUXES BY MCNPX MODELLING OF FOIL EXPERIMENTS

DAWID DE VILLIERS*, ANDY GRAHAM

Necsa, Radiation and Reactor Theory, P.O. Box 582, Pretoria, 0001, South Africa

**Email of corresponding author: dwd@necsa.co.za*

Abstract

Necsa (South African Nuclear Energy Corporation Limited) is planning an experiment to test the performance of the Pebble Bed Modular Reactor (PBMR) fuel particles at specified burn-up conditions by placing it in the SAFARI-1 core. In order to simulate the irradiations required to reach these burnups, accurate neutron fluxes are needed. To verify the SAFARI-1 core model, which is used for flux calculations, a previous cobalt and nickel foil irradiation experiment was modelled using the Monte Carlo transport code MCNPX. Neutron fluxes and reaction rates were calculated and compared with measured activity values. Results are shown and discussed.

1. Introduction

Necsa's reactor, SAFARI-1, is used for material testing applications and for the production of radioisotopes. The Radiation and Reactor Theory Group gives support to the reactor through modelling of different applications to determine radiation safety safeguards or engineering requirements. One such an application is the planned experiment to test the performance of the Pebble Bed Modular Reactor (PBMR) fuel particles at specified burn-up conditions attained by irradiating them in the SAFARI-1 core.

In order to reach the required burn-ups it is vital to know the relevant neutron fluxes and the gamma heating in the irradiation rig that will be used. Due to restrictions in the design of the irradiation rig, it is not possible to determine these parameters through measurement inside the rig. By modelling the experiment, neutron fluxes and gamma heating can be obtained both inside the irradiation rig and at locations outside, where measurements are possible. Thus the outside values can be compared to measurements and hence inside values can be estimated with greater accuracy.

In preparation for this experiment a geometrically detailed MCNPX [1] model of the SAFARI-1 core was developed that is capable of representing every single moment in a reactor cycle in terms of isotopic inventory. An interface code, OSMINT [2], manages the transfer of material data from the 3D nodal depletion code OSCAR-3 [3] to an MCNPX input template. The resulting model greatly improves previous approximations where the core was modelled as a homogenised mixture of uranium, water and aluminium [4].

The objective of this work is to verify the applicability of this SAFARI-1 core model. For the verification, an earlier cobalt and nickel foil irradiation experiment was modelled using the MCNPX core model, neutron fluxes and activities calculated and compared with the measurements.

2. Modelling with MCNPX

An MCNPX input deck of the reactor at a thermal power of 20 MW was constructed, using the OSCAR-3 program and the OSMINT interface program, representing the status of the core at the time of the foil irradiations. The exact geometry of the irradiation rig (foils and the foil holders) was obtained from engineering drawings and defined as a separate object inside the core (see Fig 1.).

The calculation was run as a KCODE source problem for criticality calculations on MCNPX v2.5. The ENDF VI (60c.) cross-section data set was used for all the radioisotopes when available; when absent, the alternate older ENDF V (50c) was used. Using 25000 k-effective cycles, the foils were tallied with F4 tallies for neutron flux and reaction rate.

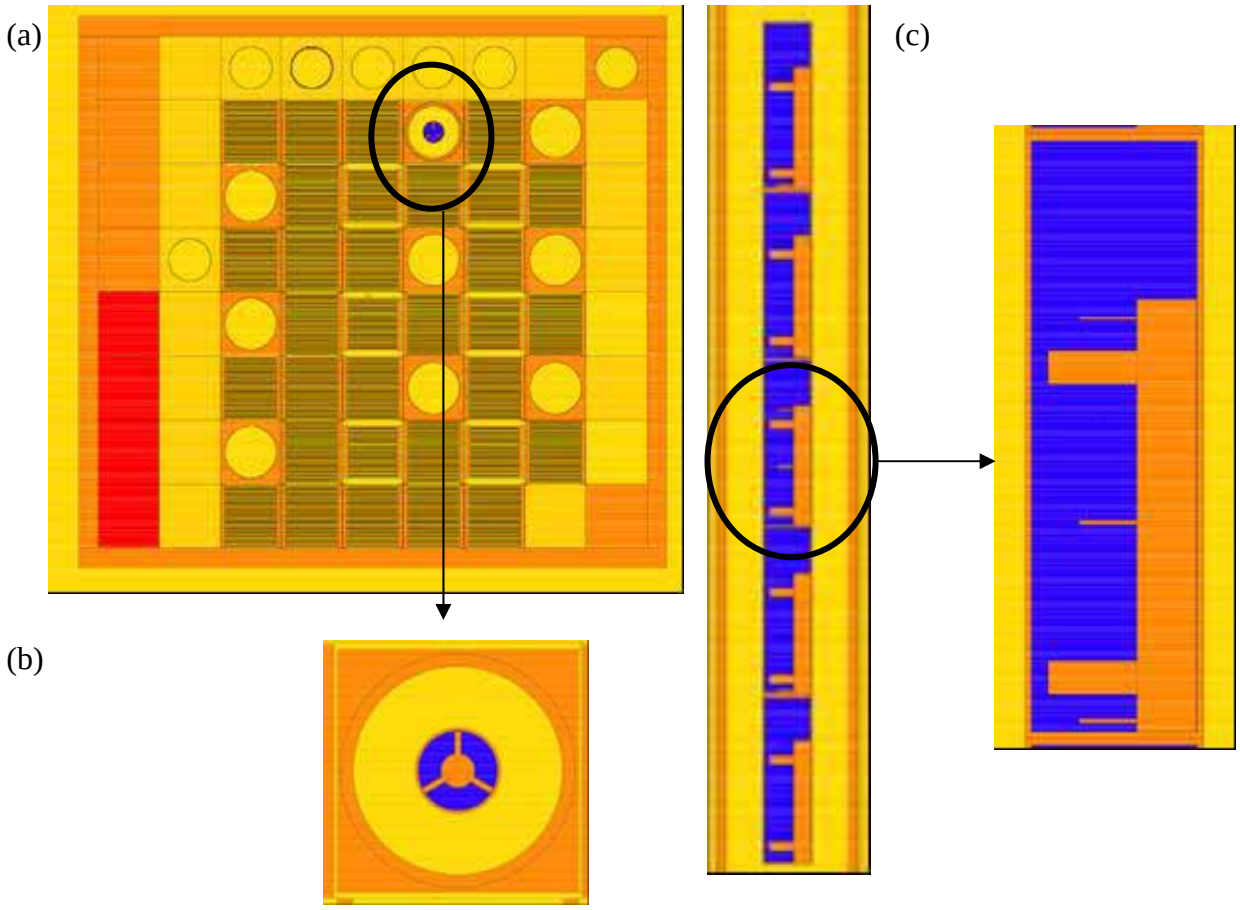

Fig 1. An illustration of the SAFARI-1 core model, with (a) the flux monitoring irradiation rig inside, (b) close up of the rig, (c) vertical view of the irradiation rig that consists of 5 foil holders and (d) close up of one foil holder with three foils.

3. Results and Discussion

Using the calculated reaction rates and fluxes, the activities (A_i) of all the foils were determined by

$$A_i = n\sigma\phi(1-e^{-\lambda t}) \ , \qquad 1.$$

with n the number of atoms, σ the absorption cross section, ϕ the neutron flux and the bracket term a decay correction factor. These and the measured values are tabulated in Table 1.

Good agreement is seen between the measured and calculational data sets (a graphical comparison between the sets of data is depicted in Fig 2 and Fig 3). For the nickel foils only two points do not show agreement. It is unsure whether it can be attributed to statistics or to modelling. However, a possibility for errors occurs when doing modelling, as only a snapshot of the actual experiment is investigated and not the total experiment. The core depletion process can therefore have an effect on the results. From the results it is concluded that the core model shows promise as a tool to aid the PBMR irradiation experiment.

Position from core centre line	Co foil activity (Bq)		Ni foil activity (Bq)	
	Measured	Calculated	Measured	Calculated
219.9	7.86E+02	8.88E+02	2.86E+05	2.75E+05
188.9	9.32E+02	1.02E+03	3.54E+05	3.71E+05
158.9	1.13E+03	1.18E+03	4.18E+05	4.41E+05
128.4	1.35E+03	1.45E+03	4.84E+05	4.98E+05
97.4	1.57E+03	1.76E+03	5.97E+05	6.57E+05
67.4	1.75E+03	1.94E+03	6.17E+05	6.11E+05
36.9	1.80E+03	2.14E+03	7.52E+05	7.48E+05
6	1.91E+03	2.19E+03	8.12E+05	6.46E+05
-24.1	2.13E+03	2.31E+03	7.96E+05	7.89E+05
-54.6	2.20E+03	2.35E+03	8.37E+05	7.98E+05
-85.6	2.24E+03	2.33E+03	8.35E+05	9.09E+05
-115.6	2.18E+03	2.24E+03	8.10E+05	8.41E+05
-146.1	2.07E+03	2.25E+03	7.96E+05	7.74E+05
-177.1	1.91E+03	1.98E+03	7.48E+05	5.66E+05
-207.1	1.86E+03	2.05E+03	6.56E+05	6.19E+05

Table 1: The measured and calculated activities for the cobalt and nickel foils per position in the SAFARI-1 core. The measurement error and the statistical error are both 10%.

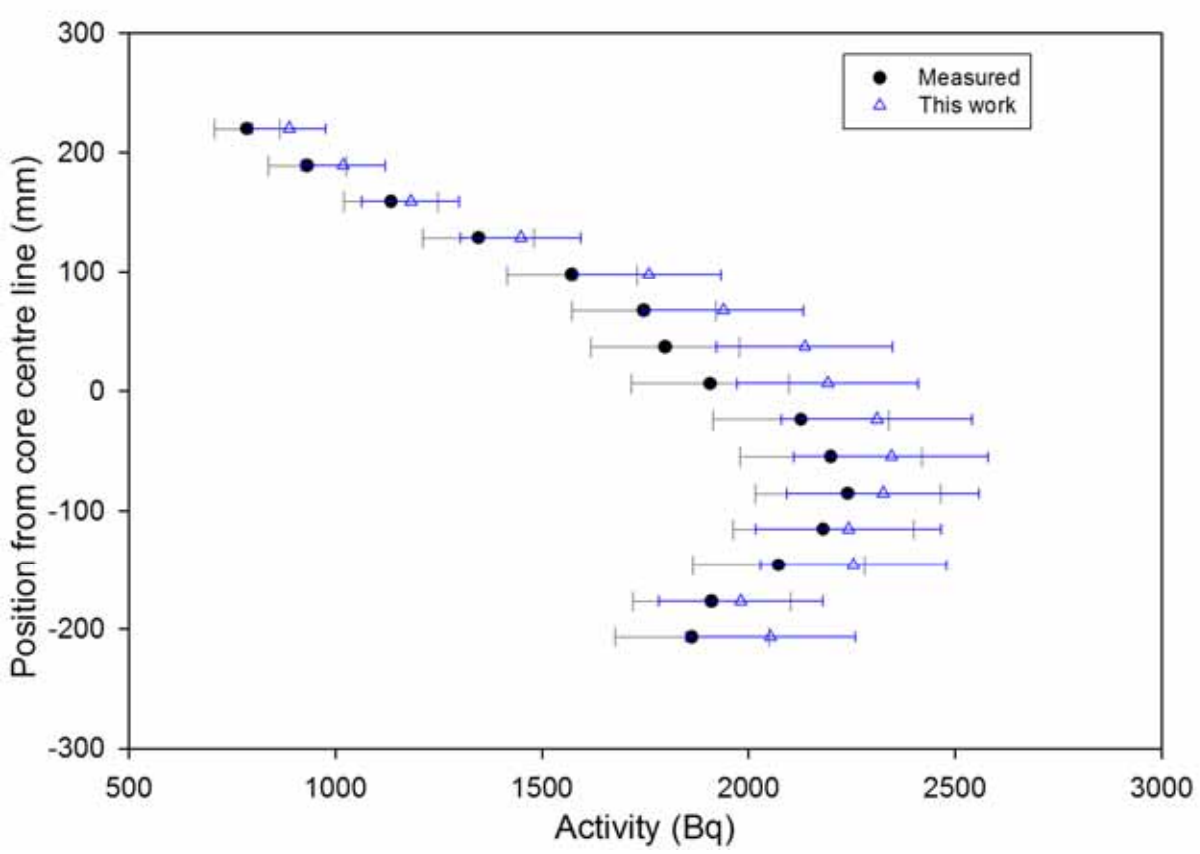

Fig 2. The measured activities compared with the calculated activities of this work for the cobalt foils as a function of position in the SAFARI-1 core.

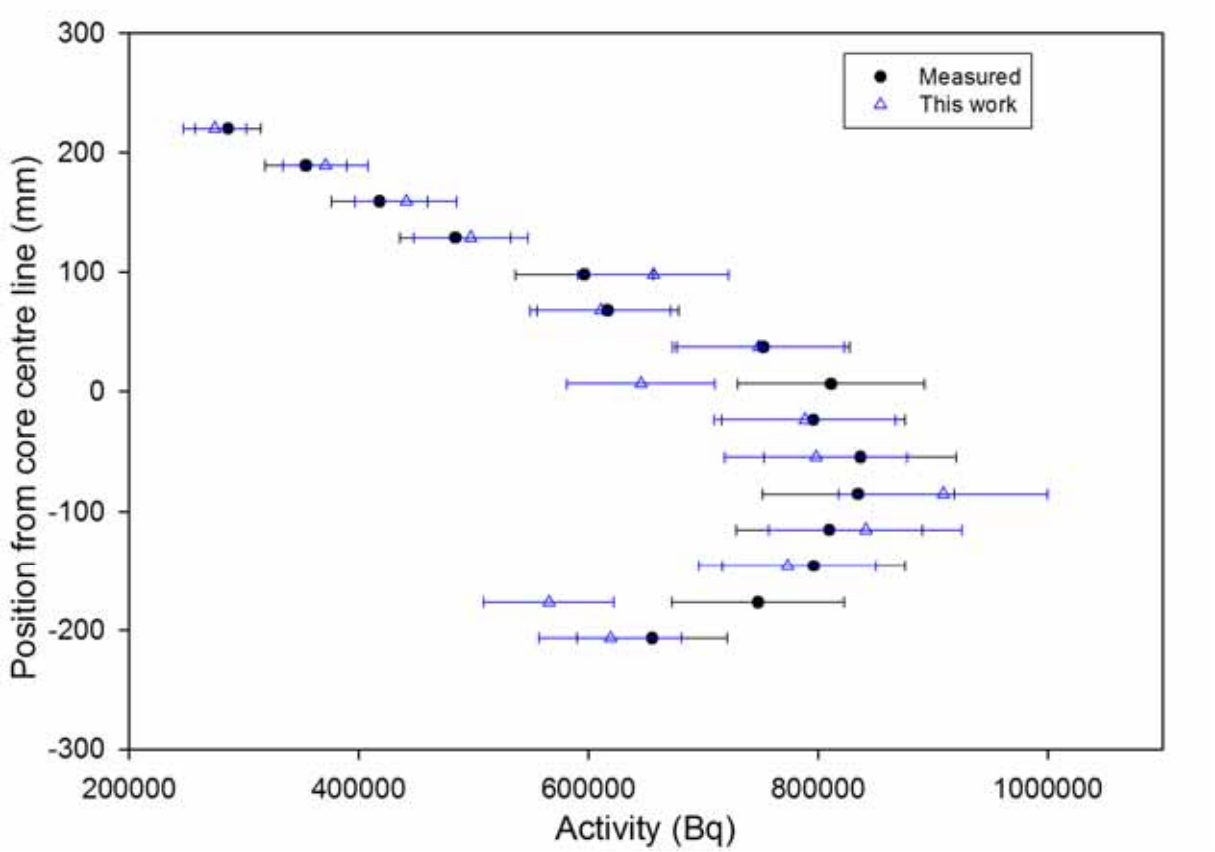

Fig 3. The measured activities compared with the calculated activities of this work for the nickel foils as a function of position in the SAFARI-1 core.

4. References

[1] Hendricks, J.S. et al. *MCNPX version 2.5*. LANL report LA-CP-05-0369, Los Alamos National Lab Los Alamos, New Mexico, April 2005.

[2] Belal, M. *OSMINT: OSCAR-3 MCNP Interface.* RRT report, Necsa, June 2006.

[3] Reitsma, F., Joubert, W.R. *A Calculational System to Aid Economical Use of MTRs*, International Conference on Research Reactor Fuel Management (RRFM '99*)*, Bruges, Belgium, March 29-31, 1999.

[4] De Villiers, D. *Shield plug thickness calculations*. RRT report RRT-SAFARI-06-4, Necsa, June 2006.

SOPHISTICATED MCNP CALCULATION OF THE FLUX MAP OF FRJ-2 USING A FULLY NODALIZED MODEL

P. BOURAUEL, R. NABBI
Research Center Jülich
Leo-Brandt-Straße, 52428 Jülich - Germany

ABSTRACT

After 44 years of operation for material research, the FRJ-2 research reactor was finally shut down on May, 2nd 2006. The running decommissioning activities which are realized according to a well defined plan, intend to place the facility in a condition that provides for the safety of the general public, decommissioning staff and the environment.
In this respect the amount of radioactive waste and radio nuclide inventory are of particular interest which are calculated on the basis of neutron flux. For the determination of the flux map the Monte-Carlo-Code MCNP was employed due to its modeling capability for high performance computing. The requirement on detailed nodalization and precise neutronic calculations results from the complex reactor construction consisting of different structures absorber layers, penetrations, beam tubes and holes. The work shows that it is possible to determine the flux distribution with a high statistical precision even for large reactor systems. Accordingly the thermal n-flux depends on the location of the components as well as on the geometry of the surrounding structures. The average thermal flux in the core, the graphite reflector, steel tank and in the inner and outer layer of the biological shield amounts to $2.0x10^{14}$, $1.7x10^{13}$, $3.2x10^{10}$, $8.7x10^{7}$ and $6.0x10^{5}$ n/cm²s respectively. Due to the streaming and scattering effects the flux around the openings is significantly higher than in the undisturbed region of the surrounding structures. The results of the calculations were produced with a reasonable computing time using the high performance computer system JUMP by employing variance reduction method.

1. Introduction

For the solution of neutron transport equation in complex systems different numerical methods are employed which are of deterministic or statistical character. In the first category mainly using the discrete ordinate method or diffusion approximation the numerical solution is performed by the definition of finite differences for a discretized geometry. Theses methods are associated with shortcomings in the representation of real geometry that may result in some uncertainties. Additional numerical uncertainties and errors may result from the use of the condensed nuclear data in few energy groups [1]. By comparison, the Monte-Carlo codes enable the user of providing the adequate flexibility in the numerical representation of complex geometries and energy domain.
Due to the complex geometry of FRJ-2 consisting of inhomogeneous structures and configuration the MCNP Monte-Carlo-code seemed to be the optimum method for precise neutronic analysis. The MCNP code is also extensively used worldwide in nuclear engineering to perform complex criticality studies and neutron and particle transport calculations [2]. It is capable of treating any 3-dimensional configuration of materials in geometric cells of complex form using pointwise continuous-energy cross sections existing for a variety of reactions [3]. The numerical models and features of the code have been extensively validated on the basis of comprehensive benchmark tests and experiments [4].
The decision for the application of MCNP was made due to the fact that a geometrical model of the reactor was existing from the sophisticated core physics investigations [5,6]. Due to the large dimension of the reactor block and limited penetration length, the model was modified by homogenizing the core region and detailed nodalization of the outer regions of the reactor. Variance reduction technique using cell importance map was applied in order to decrease uncertainties in the geometrical regions of the model, where only few neutron tracks are sampled due to large distances and shielding effects.

2. Description of FRJ-2

The FRJ-2 is a DIDO-class tank-type research reactor cooled and moderated by heavy water. The core consists of 25 tubular MTR fuel elements arranged in five rows of fuel elements. The active part of the tubular fuel elements is formed by four concentric tubes having a wall thickness of 1.5 mm and a length of 0.61 m. The reactor has been equipped with two independent and diverse shut-down systems the CCAs and the RSRs. The six CCAs are raised and lowered by angular movement around a pivot, whereas the three RSRs are shot in by pneumatic actuators.
The core is accommodated within an aluminium tank 2 m in diameter and 3.2 m in height. The tank is surrounded by a graphite reflector of 0.6 m thickness enclosed within a double-walled steel tank surrounding a lead zone as the thermal shielding with a thickness of 10 cm in which cooling tubes are installed for cooling purposes. Outside of this structure a boral layer is used to prevent neutron leakage and protect the surrounding concrete shielding (biological shield). The biological shield is a concrete blanket between the steel tank and the outer casing of the reactor. Three different kinds of heavy concrete were used in the construction. The first layer surrounding the boral layer is made of baryt concrete with boron additive.
The vertical shield of the aluminum tank and the graphite reflector is made of three layers of different thicknesses and materials namely stainless steel (1.9 cm), cadmium layer, lead (10 cm), a mild steel layer (3.8 cm) and a massive iron shot concrete in the top having a height of 70 cm. The whole tank shield has couple of holes foreseen for loading of fuel elements, which are tightened during the operation by using plugs of the same construction like the surrounding structures. Accordingly the whole reactor contains all round an absorber layer (boral) used between the thermal and biological shield. For experimental purposes a part of the boral layer and outer biological shield has been replaced by a thermal column consisting of the graphite in the peripheral zone and of steel and graphite structures at the outer region.
Due to the design of the reactor for neutron beam experiments, a high number of vertical and horizontal holes and channels have been provided in all structures and parts which penetrate from outer surfaces of the reactor block.

3. MCNP Model

The precision of the MCNP calculations is mainly determined by the modeling details of the geometrical material cells and by the uncertainties of the nuclear data as well as by the number of histories in the simulation run. The MCNP Model of the FRJ-2 is a complete 3-dimensional full-scale model with a high level of geometric fidelity representing a detailed geometrical nodalization like shown in Fig 1. Because of high interest in neutron flux in the structures outside the reactor aluminum tank the whole active core consisting of the fuel elements, part of the CCA and heavy water has been homogenized and represented as a unitary cell. This approach for the central core was applied to limit the modeling effort and achieve the necessary precision in the neutron flux calculations in the outer regions within a reasonable computing time.
For the homogenization aim, the material composition in the individual fuel elements was distributed in a cylindrical cell of the core size in accordance with the fraction of individual volumes. By this way the density of all nuclide existing in the core were determined. The core as a homogenized cell 41 cm in diameter and 60 cm high is positioned in the center of the reactor model. A second cell was generated for the zone above the core in which all aluminum tubes (for holding the fuel elements) as well as the upper structures of the CCA are homogenized.
The lower region of the core down to the bottom of the tank accommodating the grid plate, unfueled ends of the fuel elements including the aluminium structures were modelled in accordance with the design. In the whole geometric model, the cell boundaries were specified by 1st and 2nd degree surfaces with appropriate transformation in accordance with the position of the cells. The beam tubes of various diameters and lengths were modelled in detail and integrated into the entire model in accordance with the design and construction documents. Some high dimensioned material cells like the graphite reflector, thermal and biological shield, respectively, as well as the top shield with individual structures were additionally nodalized for generating tallies for a more detailed neutron flux distribution.

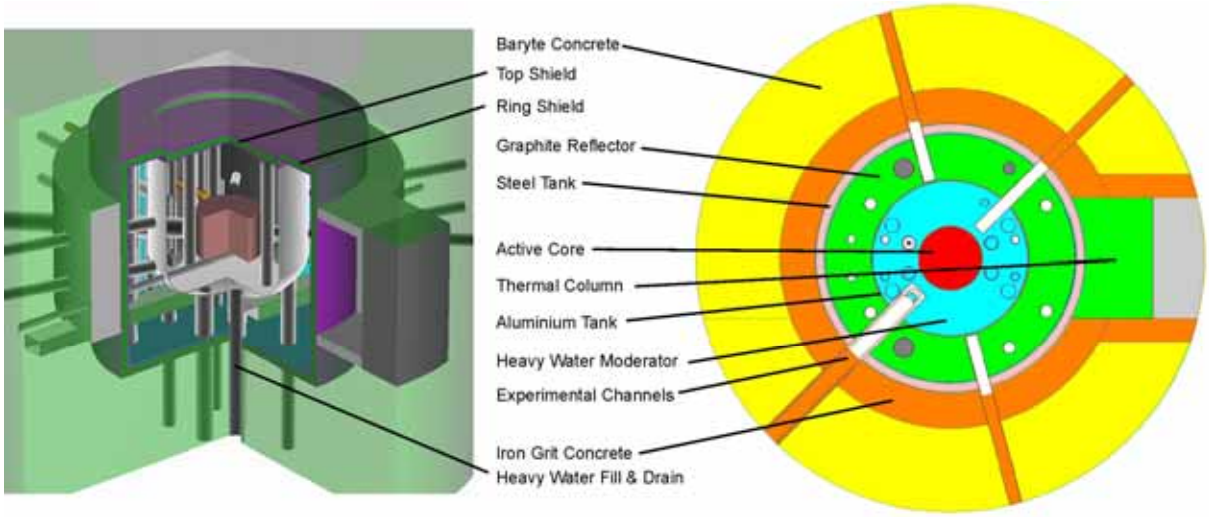

Fig 1: The MCNP model of FRJ-2 for neutron flux calculation

Due to the shielding effects and large dimension of the model, small number of neutrons is tracked in the outer regions resulting in a high statistical relative errors and low reliability on the calculated neutron flux. To improve the performance of the simulations, the variance reduction technique has been employed by the adjustment of cell importances. Using the optimized cell importances, number of neutron history was continuously increased to achieve a sufficient number of neutron tracks for a performed sampling in all cells including the outer regions. The simulations have been performed on the JUMP supercomputer operated at the Research Centre Jülich. JUMP (JUelich Multi Processor) is an IBM p690-Cluster consisting of 1312 processors in 41 nodes with 5.2 Terabytes Memory and a theoretical computation performance of 8.9 Teraflops/s.

4. Results of neutronic calculations

Due to the complexity of the geometrical model of the reactor and the large number of particle histories, the computing time was reduced significantly by the application of the parallel version of MCNP5. The simulations were carried out in steps of 5 million histories. After each step results were checked with regard to statistical errors and standard deviation and returned to MCNP by using the restart capability of the code. In total 50 Mio. histories were simulated resulting in a standard deviation (neutron flux) of less than 1 % around the graphite reflector and steel tank and up to 10 % in the inner parts of the biological shielding behind the absorber blanket. The results of a standard run in an output file are given for one source neutron in each cell of the whole model. To calculate the neutron flux for the real operating condition of the reactor the result had to be divided by the volume of the respective tally cell and multiplied with the total neutron generation rate (1.55×10^{18} n/s). This conversion factor is determined according to the nominal reactor power at which the reactor has been running during the last phase of operation before final shut down (20 MW).

To check the accuracy of the results, the neutron flux in different zones of the core and surrounding parts as well as the neutron spectrum at the boundary surface of the active core were compared with the calculations separately carried out on the basis of a detailed core model. Due to the fact that the effect of the homogeneity of the core decreases with the distance from the core, a good agreement could be found for the regions outside the aluminium tank, which are of particular interest for further analysis and determination of radioactivity inventory. The results of the final calculation are summarized in in Fig. 2 for the whole reactor block. Accordingly the neutron flux in the inner parts of the reactor, the aluminium tank, the grid plate and in the experimental channels surrounded by heavy water is significantly higher than in the outer structures. The average flux from the core to the outer structures is decreased n many orders of magnitude.

The thermal neutron flux in the steel tank with its different layers experiences a decrease in the direction of the outer regions. In this structure, the flux is ranged between 9×10^{9} n/cm²s (inside the

boral layer) and $1.2x10^{10}$ n/cm²s in the outer steel casing. Due to the simulation of high number of histories the relative error of the flux calculation is less than 1 % (1σ). The highest flux in the heavy concrete of the biological shield behind the steel tank is found to be $8.7x10^{7}$ n/cm²s. For some parts of the biological shield the flux decreases with the increase of distance to a level, where the statistical error exceeds 15% due to the low number of neutron tracks. For these few zones (outer boundary zones) the thermal neutron flux was determined by an analytical attenuation calculation using the neutron flux distribution in the surrounding region.

The neutron flux in the structures containing beam tubes and channels is significantly influenced by neutron streaming through the holes. The result is an increase of the flux in the backside structure (Fig 3) around the channel. This effect is clearly demonstrated in Fig. 3 representing the flux pattern in the steel tank over the whole surface. The streaming effect causes a flux profile around the opening which gradually decreases. According to the results the background flux is reached at a distance of three times the geometrical radius. The simulation reveals the same phenomenon behind an absorber layer with distributed cut-outs.
In the top shield, the thermal neutron flux is about $2x10^{11}$ n/cm²s for the lower stainless steel plate, which falls in the upper parts of the heavy concrete under 10^{5} n/cm²s. The relative error of the simulation remains limited to less 10 % in the lower components of the top shield. For the upper parts of the top shield consisting of iron shot concrete it was possible to increase the precision of the simulation by the modification of the cell importances as a variance reduction method. The thermal flux in the lower layer of the concrete shield amounts to $5.8x10^{7}$ n/cm²s, which falls three orders of magnitude. Due to lack of absorber layer in front of the thermal column higher values for the neutron flux are obtained in this structure as well as in the fill and drain Ducts. Using the same approach for certain cells in the outer biological shield, a considerable calculation performance expressed in computational time and precision could be achieved. In view of the decommissioning process of FRJ-2 the existing distribution of the flux allows the determination of the detailed activity inventory in the individual components and structures as well as the radiation dose.

6. References

[1] LEWIS, E. E.; ET AL: COMPUTATIONAL METHODS OF NEUTRON TRANSPORT, A WILEY-INTERSCIENCE PUBLICATION, JOHN WILEY AND SONS, INC., 1984.

[2] BRIESMEISTER, J.F.: MCNP 4A MONTE CARLO N-PARTICLE TRANSPORT CODE SYSTEM, RSICC, LOS ALAMOS, 1994, CCC-0200

[3] R. D. MOSTELLER; ET AL: DATA TESTING OF ENDF/B-VI WITH MCNP: CRITICAL EXPERIMENTS, REACTOR LATTICES AND TIME-OF-FLIGHT MEASUREMENTS, ADVANCES IN NUCL. SCI. AND TECHN., 1998, VOL. 24

[4] F. RAHNEMA; ET AL: COMPARISON OF ENDF/BV AND VI.3 FOR WATER REACTOR CALCULATIONS PROC. ANN. MTG. OF AMERICAN NUCLEAR SOCIETY, VOL. 76, PP. 324-325, JUNE 1997

[5] NABBI, R.; WOLTERS, J.: COUPLING MCNP AND A DEPLETION CODE FOR DETAILED NEUTRONIC ANALYSIS AND OPTIMUM CORE MANAGEMENT AT THE GERMAN FRJ-2 RESEARCH REACTOR, INTERNATIONAL MEETING ON: MATH. METHODS FOR NUCLEAR APPLICATIONS, SALT LAKE, USA, SEPT. 2001

[6] NABBI, R.; BERNNAT, W.: APPLICATION OF COUPLED MONTE CARLO AND BURN-UP METHOD FOR DETAILED NEUTRONIC ANALYSIS FOR THE FRJ-2 RESEARCH REACTOR ON HIGH PERFORMANCE COMPUTERS, INTERN. CONFERENCE ON THE MONTE CARLO METHOD:, CHATTANOOGA, USA, APRIL, 2005, AMERICAN NUCLEAR SOCIETY

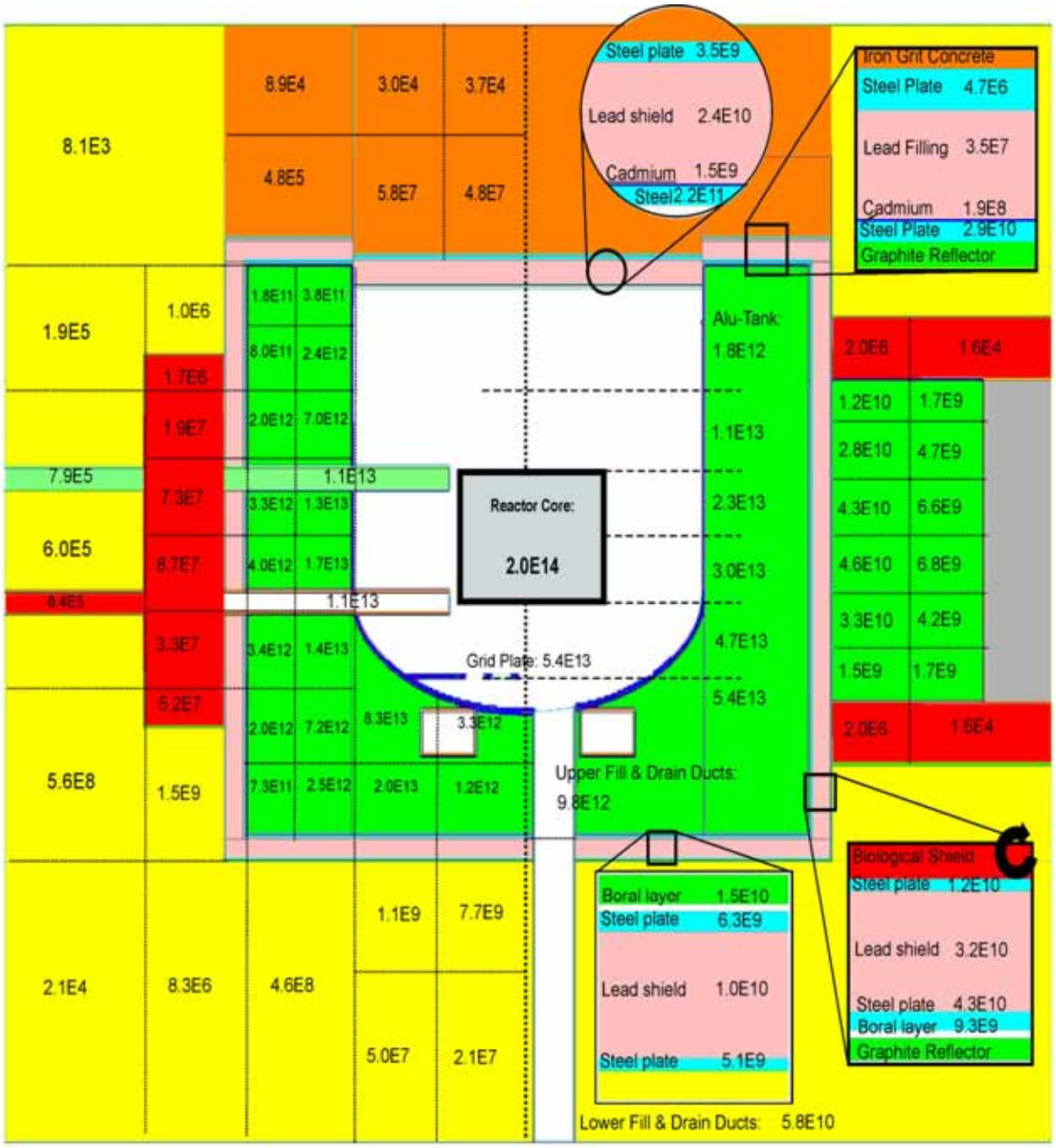

Fig 2: Results of the FRJ-2 neutron flux calculations using MCNP [n/cm²s]

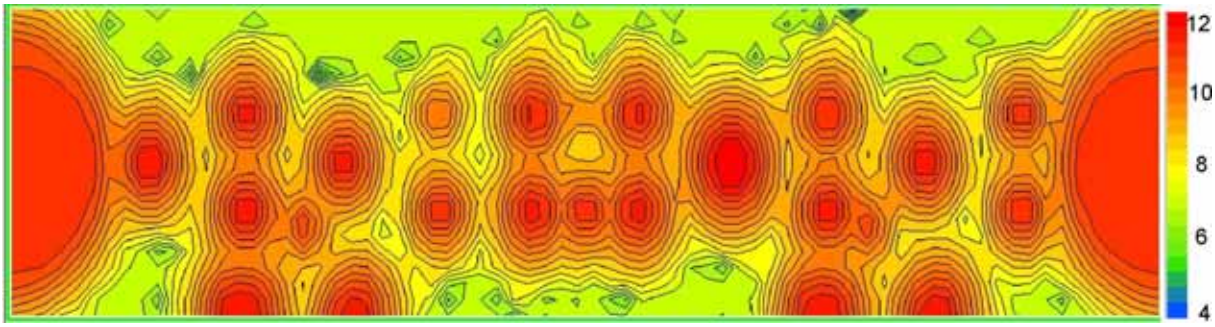

Fig 3: The distribution of neutron flux in the thermal shield behind the boral layer [log(n/cm²s)]

RRFM IGORR 2007

LYON, France 11.3. - 15.3. 2007

European Nuclear Society
Rue de la Loi 57
1040 Brussels, Belgium
Telephone +32 2 505 30 54
Fax + 32 2 502 39 02
rrfm2007@euronuclear.org
www.euronuclear.org

Layout and Design: Marion Brünglinghaus, ENS